Journal of Medicinal Chemistry

Article

pubs.acs.org/jmc

Enantiomerically Pure 2-Methyltetrahydro-3-benzazepin-1-ols Selectively Blocking GluN2B Subunit Containing *N*-Methyl-D-aspartate Receptors

Bastian Tewes,[†] Bastian Frehland,[†] Dirk Schepmann,[†] Dina Robaa,[‡] Tanaporn Uengwetwanit,[‡] Friedemann Gaube,[§] Thomas Winckler,[§] Wolfgang Sippl,[‡] and Bernhard Wünsch*[,†,∥]

[†]Institut für Pharmazeutische und Medizinische Chemie der Universität Münster, Corrensstraße 48, D-48149 Münster, Germany

[‡]Institut für Pharmazie, Martin-Luther-Universität Halle-Wittenberg, Wolfgang-Langenbeck-Strasse 4, D-06120 Halle/Saale, Germany

[§]Institut für Pharmazie der Friedrich-Schiller-Universität Jena, Semmelweisstraße 10, D-07743 Jena, Germany

[∥]Cells-in-Motion Cluster of Excellence (EXC 1003-CiM), Universität Münster, 48149 Münster, Germany

Supporting Information

ABSTRACT: A chiral pool synthesis was developed to obtain all four stereoisomeric 2-methyl-3-(4-phenylbutyl)tetrahydro-3-benzazepin-1-ols **21**, **31**, and **32** in a seven- to eight-step sequence. The phenols **32** reveal slightly higher GluN2B affinity than the methyl ethers **21**. The GluN2B affinity increases in the order (1*R*,2*S*) < (1*S*,2*S*) < (1*S*,2*R*) < (1*R*,2*R*). The stereoisomeric phenols (*R*,*R*)-**32** and (*S*,*R*)-**32** show the highest GluN2B affinity and the highest cytoprotective activity. Both compounds represent GluN2B selective allosteric NMDA receptor antagonists. Docking of the 3-benzazepin-1-ols into the ifenprodil binding site of the crystallized GluN1b/GluN2B N-terminal domains led to free binding energies, which correlate nicely with the experimentally determined GluN2B affinities. The similar GluN2B affinity of the stereoisomeric phenols (*S*,*S*)-**32**, (*R*,*R*)-**32**, and (*S*,*R*)-**32** is explained by different binding modes of the 3-benzazepine scaffold. The benzyl ethers **31** reveal unexpectedly high GluN2B affinity but do not show cytoprotective effects. The additional benzyl moiety of **31** binds into a previously unrecognized lipophilic subpocket.

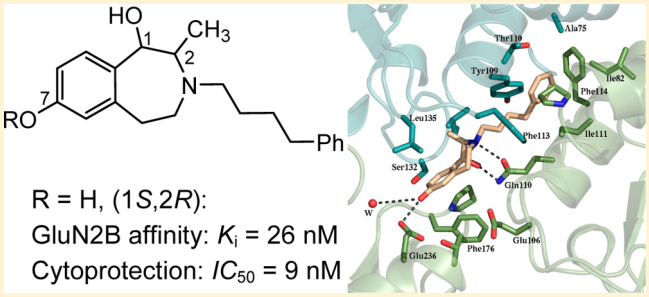

INTRODUCTION

The most important excitatory neurotransmitter in the central nervous system is the amino acid (*S*)-glutamate. This neurotransmitter mediates its effects via activation of metabotropic (mGlu) and ionotropic glutamate receptors (iGlu). According to their sequence homology, their signal transduction pathway, and their ligand binding profile, the G-protein-coupled metabotropic glutamate receptors are subdivided into three groups: group I contains the receptor subtypes mGlu1 and mGlu5; group II contains the subtypes mGlu2 and mGlu3, and the residual metabotropic glutamate receptors mGlu4, mGlu6, mGlu7, and mGlu8 belong to group III metabotropic glutamate receptors. In the field of ionotropic glutamate receptors three subtypes have been identified, which were termed according to their prototypical ligands: *N*-methyl-D-aspartate gave name to the NMDA receptor; 2-amino-3-(5-hydroxy-2-methylisoxazolyl)propionic acid is the prototypical ligand for the AMPA receptor; the natural product kainic acid isolated from Japanese red algae was the first compound that activated kainate receptors.[1,2]

The NMDA receptor is characterized by four particular features: (1) at normal membrane potential the receptor is blocked by Mg^{2+} ions. In order to open the channel, the Mg^{2+} block has to be removed by predepolarization of the surrounding neuronal membrane, e.g., by activation of AMPA or kainate receptors adjacent to the NMDA receptor. (2) Activation of the NMDA receptor requires two agonists, (*S*)-glutamate and the so-called coagonist glycine. (3) The NMDA receptor controls the influx of Ca^{2+} ions. The physiological concentration of Ca^{2+} ions is important for the development of neurons, but an increased intracellular Ca^{2+} ion concentration is associated with damage of neurons (excitotoxicity). (4) In addition to the agonists (*S*)-glutamate and glycine, several other small molecules are able to modulate the opening state of the NMDA receptor by interacting with particular binding sites. The receptor contains binding sites for phencyclidine (PCP) within the ion channel, Zn^{2+} ions, protons, NO, polyamines, and ifenprodil (**1**) at the amino terminal part of the receptor protein.[1,2]

The NMDA receptor is a heterotetrameric protein. Cloning of the different NMDA receptor subunits led to seven proteins, which are classified into three types of subunits: GluN1 subunit with eight splice variants termed GluN1a–h, four GluN2 and

Received: June 11, 2015

DOI: 10.1021/acs.jmedchem.5b00897
J. Med. Chem. XXXX, XXX, XXX−XXX

two GluN3 subunits encoded by different genes and termed GluN2A−D and GluN3A,B, respectively. A functional NMDA receptor protein contains at least one GluN1 subunit bearing the glycine binding site and one GluN2 subunit bearing the (*S*)-glutamate binding site.[3−5]

Herein we focus on novel ligands for the ifenprodil binding site of the NMDA receptor. The ifenprodil binding site is special because it is located at the interface between the N-terminal domains of the GluN2B and GluN1 subunits.[6] The N-terminal domains of GluN2A and GluN2B subunits, which have a clamshell-like structure, are responsible for the correct subunit assembly.[6,7] Whereas the GluN1 subunits are expressed ubiquitously throughout the central nervous system, the expression of the GluN2 subunits depends on the age and the region of the human brain. For example, the GluN2B subunit is widely expressed in the prenatal brain, but in the adult brain it is found predominantly in the cortex, striatum, and hippocampus. The amount of the GluN2B subunit in the adult cerebellum is rather low, while GluN2C subunits are expressed predominantly in this region of the brain.[8] Ligands modulating the opening state of NMDA receptors by interaction with the ifenprodil binding site selectively address GluN2B containing NMDA receptors but do not influence the activity of the NMDA receptors containing GluN2A, GluN2C, and GluN2D subunits, which leads to an optimized side effect profile.[9]

Compounds blocking GluN2B containing NMDA receptors (GluN2B antagonists) by interacting with the ifenprodil binding site have a high neuroprotective potential, which can be exploited for the treatment of traumatic brain injury, stroke (cerebral ischemia), neuropathic pain,[10] and Parkinson's disease. Moreover, GluN2B antagonists could be useful for the therapy of migraine, depression, and alcohol withdrawal symptoms.[1,2,8]

In the 1990s it was shown that **1** (ifenprodil), which was originally developed as α_1 receptor antagonist, inhibits selectively GluN2B containing NMDA receptors (IC_{50} = 13.3 nM) (Figure 1).[11] The low selectivity of **1** addressing

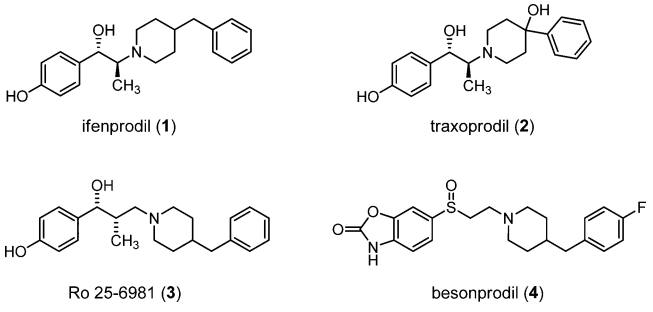

Figure 1. Prominent GluN2B antagonists.

additionally some types of Ca^{2+} channels, 5-HT_{1A}, 5-HT_2, α_1, σ_1, and σ_2 receptors led to side effects (e.g., psychotomimetic effects, memory deficit, hypertension). Moreover, the low bioavailability of **1** was due to fast metabolic degradation.[12] Nevertheless **1** has served as a lead compound for the development of potent, selective, and bioavailable GluN2B containing NMDA receptor antagonists. In Figure 1 the prominent GluN2B antagonists traxoprodil (**2**), Ro 25-6981 (**3**), and besonprodil (**4**) derived from **1** are shown.[13] **2** was studied in phase II clinical studies for the treatment of traumatic brain injury. Because of lack of efficacy, the development of **2** was discontinued, although it showed an excellent side effect profile.[14] However, the promising neuroprotective effects of these compounds in animal assays (e.g., model of Parkinson's disease)[15] stimulated the further development of GluN2B antagonists.

Binding of **1** and its analogs to the NMDA receptor takes place in a special binding site, which is termed ifenprodil binding site. GluN1 and GluN2B N-terminal domains form heterodimers, where residues lining the dimer interface construct the binding pocket for the phenylethanolamine derivatives. As can be seen from the crystal structures of the heterodimer of the N-terminal domains of GluN1b and GluN2B subunits in complex with **1** or its analog **3** (PDB codes 3QEL and 3QEM; respectively), key polar and hydrophobic interactions participate in the stabilization of the antagonists in their binding pocket.[6] These interactions are discussed in detail in the section Molecular Modeling Studies.

Recently we have reported on the synthesis and pharmacological evaluation of tetrahydro-3-benzazepines **5**−**7**, which show high affinity to the ifenprodil binding site of GluN2B containing NMDA receptors. The phenol **5** results from a formal rearrangement of **1**, i.e., disconnection of the C-3/C-4-bond of the piperidine ring and reconnection of the free methylene moiety to the benzene ring (Figure 2). Introduction

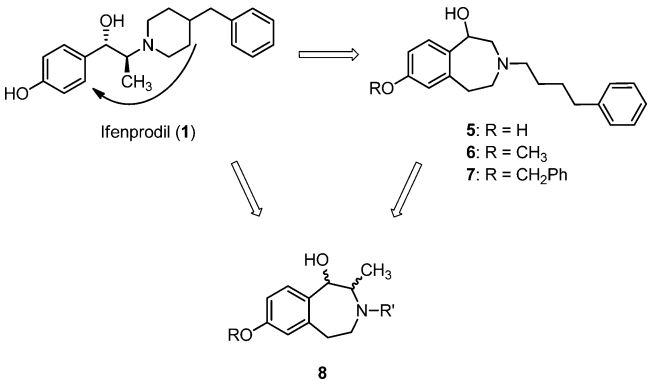

Figure 2. Development of the methylated 3-benzazepinols **8**.

of the flexible phenylethylamine part of **1** into the 3-benzazepine scaffold of **5** retains high GluN2B affinity (K_i(**5**) = 14 nM) but increased the receptor selectivity. The methyl ether **6** represents an even more affine and selective GluN2B antagonist (K_i(**6**) = 5.4 nM) but showed reduced antagonistic effects. The GluN2B affinity of the benzyl ether **7** was considerably reduced (K_i(**7**) = 187 nM).[16,17]

A comparison of the 3-benzazepines **5**−**7** with the lead compound **1** shows that the methyl moiety in β-position to the OH moiety of **1** is missing. In order to investigate the role of this methyl moiety on the GluN2B affinity, we planned to synthesize and pharmacologically evaluate 3-benzazepines **8** with an additional methyl moiety in β-position to the OH group. Since the 3-benzazepines of type **8** contain two centers of chirality, a stereoselective synthesis of all four stereoisomers was envisaged.

SYNTHESIS

For the synthesis of 3-benzazepines **8**, a chiral pool synthesis was envisaged using the enantiomerically pure proteinogenic amino acid (*S*)-alanine ((*S*)-**11**) as the starting material (Scheme 1). Esterification of (*S*)-**11** with methanol and

DOI: 10.1021/acs.jmedchem.5b00897
J. Med. Chem. XXXX, XXX, XXX−XXX

Scheme 1[a]

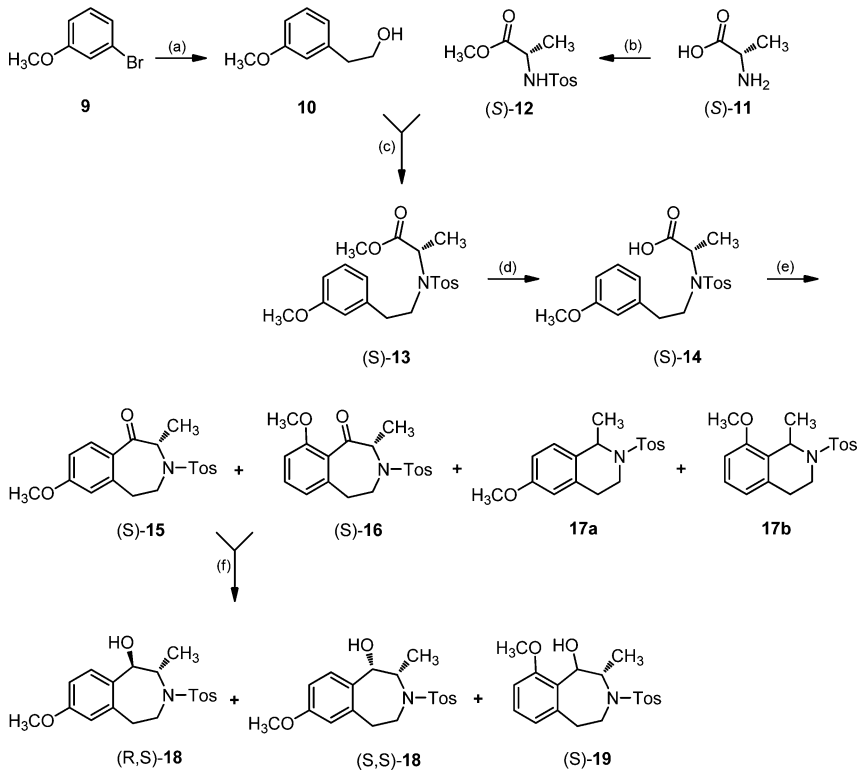

[a]Reagents and reaction conditions: (a) (1) *n*-BuLi, THF, −78 °C, 2 h; (2) ethylene sulfate, THF, −78 °C → rt, 16 h; (3) H_2SO_4, H_2O, 47 h, Δ, 62%.[21] (b) (1) CH_3OH, $SOCl_2$, rt, 2 h, 95%; (2) TosCl, CH_2Cl_2, Et_3N, rt, 20 h, 73%. (c) (*S*)-**12**, THF, 0 °C, then **10**, PPh_3, DIAD, 0 °C, 1 h, rt, 16 h, 91%. (d) LiOH·H_2O, THF/H_2O (7:3), rt, 24 h, 87%. (e) Trifluoroacetic acid anhydride ($(CF_3C{=}O)_2O$), $SnCl_4$, CH_2Cl_2, −30 °C, 22 h. (f) $LiBH_4$, THF, −90 °C, 24 h. The enantiomers (*S*,*R*)-**18** and (*R*,*R*)-**18** were prepared in the same manner starting with (*R*)-configured sulfonamide (*R*)-**12**[22] prepared from (*R*)-configured alanine (*R*)-**11**.

subsequent reaction with tosyl chloride led to the N-tosylated methyl ester (*S*)-**12**,[18,19] which should be alkylated with the phenylethanol derivative **10** in a Mitsunobu reaction.[20] Phenylethanol **10** was prepared very efficiently from bromobenzene **9** in a one-pot, three-step procedure comprising bromine−lithium exchange, reaction of the resulting aryllithium intermediate with cyclic ethylene sulfate, and hydrolysis of the sulfuric acid hemiester intermediate.[21] The Mitsunobu reaction of the secondary sulfonamide (*S*)-**12** with the alcohol **10** using PPh_3 and diisopropyl azodicarboxylate (DIAD) provided the tertiary sulfonamide (*S*)-**13** in 71% yield. The preparation of the enantiomer (*R*)-**13** was supported by microwave irradiation giving the (*R*)-configured sulfonamide (*R*)-**13** in 67% yield. Alkylation of the sulfonamide (*S*)-**12** with the corresponding phenylethyl iodide or phenylethyl tosylate provided the tertiary sulfonamide (*S*)-**13** only in very low yields (0−18%). In order to avoid racemization, the hydrolysis of the ester (*S*)-**13** was performed very carefully using LiOH at room temperature to afford the acid (*S*)-**14** in 87% yield.

The intramolecular Friedel−Crafts acylation of the carboxylic acid (*S*)-**14** was performed with P_4O_{10} in CH_2Cl_2 analogously to the cyclization of the nonmethylated analog.[16] Unexpectedly, the desired compounds (*S*)-**15** and (*S*)-**16** with a seven-membered ring were formed in only 4% yield, while the corresponding isoquinolines **17** predominated (19% yield). Several reaction conditions (see Table SI-1 in Supporting Information) were investigated to improve the yield of this key step, and finally it was found that transformation of the carboxylic acid (*S*)-**14** with trifluoroacetic acid anhydride $(CF_3CO)_2O$ into a mixed anhydride and subsequent cyclization with $SnCl_4$ provided 60% of a 1:1 mixture of the 3-benzazepines (*S*)-**15** and (*S*)-**16** and only small amounts of isoquinolines **17**.

As the regioisomeric 3-benzazepines (*S*)-**15** and (*S*)-**16** could not be separated by flash chromatography, the mixture was reduced with $LiBH_4$ at −90 °C and the resulting alcohols were separated and isolated in 25% ((*R*,*S*)-**18**), 19% ((*S*,*S*)-**18**), and 51% ((*S*)-**19**) yields, respectively.

The final reaction steps comprised removal of the tosyl protective group of (*R*,*S*)-**18** and (*S*,*S*)-**18** with magnesium in methanol and alkylation of the secondary amines (*R*,*S*)-**20** and (*S*,*S*)-**20** with 1-chloro-4-phenylbutane to yield the diastereomeric 3-benzazepines (*R*,*S*)-**21** and (*S*,*S*)-**21** (Scheme 2). The corresponding enantiomers (*S*,*R*)-**21** and (*R*,*R*)-**21** were prepared in the same manner starting with (*R*)-alanine ((*R*)-**11**).

The enantiomeric purity of the final compounds **21** was analyzed by chiral HPLC (Chiralpak AD). It was shown that about 25% racemization had occurred during the synthesis (Table SI-2). We assume that the intramolecular Friedel−Crafts acylation of (*S*)-**14** and (*R*)-**14** is responsible for the racemization. In order to test enantiomerically pure compounds, the 3-benzazepines **21** were purified by preparative chiral HPLC. Finally the four stereoisomers (*R*,*S*)-**21**, (*S*,*S*)-**21**, (*S*,*R*)-**21**, and (*R*,*R*)-**21** were isolated with an enantiomeric purity greater than 99.1:0.9 (Table SI-2, Figure SI-1A−D).

The relative configuration of the 3-benzazepines **18**, **20**, and **21** could not be assigned unequivocally by analysis of the

DOI: 10.1021/acs.jmedchem.5b00897
J. Med. Chem. XXXX, XXX, XXX−XXX

Scheme 2[a]

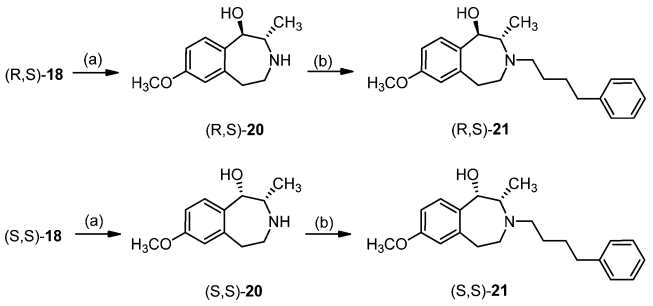

[a]Reagents and reaction conditions: (a) Mg, CH_3OH, Δ, 16 h. (b) 1-Chloro-4-phenylbutane, CH_3CN, Bu_4NI, K_2CO_3, Δ, 72 h. The enantiomers (*S*,*R*)-**21** and (*R*,*R*)-**21** were prepared in the same manner starting with (*S*,*R*)-**18** and (*R*,*R*)-**18**.

coupling constants in the NMR spectra because of undefined dihedral angles in the flexible seven-membered ring system. Therefore, X-ray crystal structures of (*S*,*R*)-**21** (42% ee) and (*R*,*R*)-**21** (52% ee) were recorded.[23] The X-ray crystal structure (Figure SI-4) clearly shows *trans*-configuration of the OH moiety and the methyl group, proving unlike-configuration of (*S*,*R*)-**21** (42% ee). On the other hand *cis*-orientation of these substituents is displayed in Figure SI-5, proving like-configuration of (*R*,*R*)-**21** (52% ee).

In addition to the four diastereomeric methyl ethers **21**, the corresponding phenols **32** were prepared and tested. For this purpose the methyl ether of the ketone (*S*)-**15** should be cleaved in analogy to the cleavage of the corresponding nonmethylated analog.[17] However, all attempts using $AlCl_3$, BBr_3, or $LiBH(sec\text{-}Bu)_3$ failed to give the corresponding phenol. Therefore, the synthesis of the 3-benzazepine scaffold was repeated with different phenol protective groups.

Thus, the phenolic OH moiety of 3-/2-hydroxyethyl)phenol (**22a**) was converted selectively into the benzyl ether **22b**, the *p*-methoxybenzyl ether **22c**, and the triisopropylsilyl ether **22d** (Scheme 3). Mitsunobu reaction of the different ethers **22b–d** with the alanine derived sulfonamide (*S*)-**12** afforded the coupling products (*S*)-**23b–d** in 71–78% yields, which were hydrolyzed with LiOH to obtain the carboxylic acids **24b–d**. Whereas the carboxylic acids (*S*)-**24b** and (*S*)-**24c** with benzyl protective groups were obtained in 73% and 96% yields, respectively, the triisopropylsilyl protected phenol (*S*)-**24d** gave only 35% yield indicating the instability of the phenyl silyl ether.

The intramolecular Friedel–Crafts acylation of the benzyl ether (*S*)-**24b** using $(CF_3C{=}O)_2O$ and $SnCl_4$ as for the cyclization of the methyl ether (*S*)-**14** led to a mixture of the cyclic ketones (*S*)-**25b** and (*S*)-**26b** in 20% yield (Scheme 3). Additionally the O-debenzylated 3-benzazepines (*S*)-**25a** and (*S*)-**26a** (10% yield) and the O-debenzylated isoquinoline **27a** (7% yield) were isolated. Obviously a fast debenzylation had occurred under the Lewis acid catalyzed Friedel–Crafts acylation conditions. In order to increase the yield of the benzyl protected 3-benzazepinone (*S*)-**25b**, the crude reaction mixture was treated with benzyl bromide and K_2CO_3 to convert the phenol (*S*)-**25a** into the benzyl ether (*S*)-**25b**. After several optimization experiments including the subsequent benzylation of the free phenol (*S*)-**26a**, a 95:5 mixture of regioisomeric 3-benzazepinones (*S*)-**25b** and (*S*)-**26b** was isolated in 41% yield. The higher regioselectivity of the cyclization of the benzyl ether (*S*)-**24b** compared to the cyclization of the methyl ether (*S*)-**14** is explained by shielding the *o*-position by the larger benzyloxy moiety.

Cyclization of the *p*-methoxybenzyl ether (*S*)-**24c** using the optimized reaction conditions ($(CF_3C{=}O)_2O$, $SnCl_4$) led also to considerable cleavage of the *p*-methoxybenzyl ether and provided, after treatment of the crude reaction product with *p*-methoxybenzyl bromide and K_2CO_3, a 30:70-mixture of the regioisomeric 3-benzazepinones (*S*)-**25c** and (*S*)-**26c** in 25% yield (Scheme 3). After reaction of the silyl ether (*S*)-**24d** with $(CF_3C{=}O)_2O$ and $SnCl_4$, the silyl ether (*S*)-**25d** and the phenol (*S*)-**26a** were isolated in 18% and 7% yields, respectively. In this case only the silyl ether in *o*-position to the ketone ((*S*)-**26d**) was cleaved, whereas the corresponding regioisomeric silyl ether (*S*)-**25d** remained intact. Finally the phenol (*S*)-**24a**, which was obtained by hydrogenolytic cleavage of the benzyl ether (*S*)-**24b**, was cyclized with $(CF_3C{=}O)_2O$ and $SnCl_4$ to yield 9% of the desired 3-benzazepinone (*S*)-**25a** and 11% of the ring-contracted isoquinoline **27a**; the corresponding 9-hydroxy-3-benzazepinone (*S*)-**26a** could not be detected.

Since the cyclization of the benzyl ether (*S*)-**24b** gave the highest yield of the 3-benzazepinones (41%) and the best regioselectivity (95:5), the 95:5 mixture (*S*)-**25b**/(*S*)-**26b** was

Scheme 3[a]

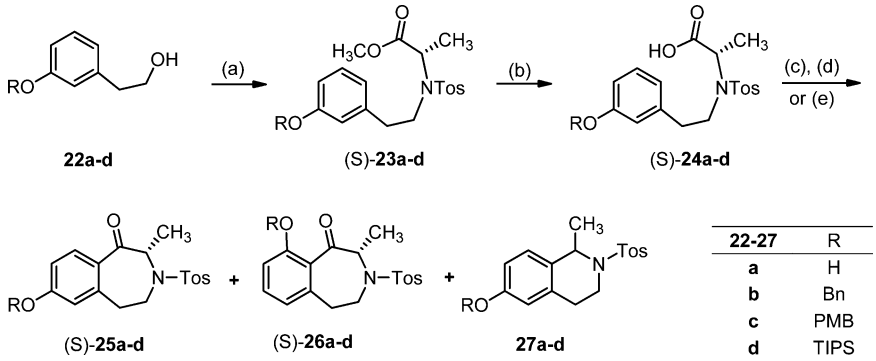

[a]Reagents and reaction conditions: (a) (*S*)-**12**, DIAD, Ph_3P, THF, 0 °C → rt, 18 h. (b) $LiOH{\cdot}H_2O$, THF/H_2O (7:3), rt, 16 h. (c) (**24b**) $SnCl_4$, trifluoroacetic acid anhydride, CH_2Cl_2, −15 °C, 23 h, then benzyl bromide, acetone, K_2CO_3, Δ, 6 h. (d) (**24c**) $SnCl_4$, trifluoroacetic acid anhydride, CH_2Cl_2, −15 °C, 23 h, then 4-methoxybenzyl bromide, acetone, K_2CO_3, Δ, 6 h. (e) (**24d**) $SnCl_4$, trifluoroacetic acid anhydride, CH_2Cl_2, −15 °C, 23 h. The enantiomers (*R*)-**25b** and (*R*)-**26b** were prepared in the same manner starting with (*R*)-**12**.

DOI: 10.1021/acs.jmedchem.5b00897
J. Med. Chem. XXXX, XXX, XXX–XXX

further processed to access the final GluN2B antagonists. Reduction with $NaBH_4$ afforded the diastereomeric alcohols (*R*,*S*)-**28** and (*S*,*S*)-**28** as well as the regioisomeric alcohol **29**, which were separated and purified by flash chromatography (Scheme 4). Removal of the tosyl group from (*R*,*S*)-**28** and

Scheme 4[a]

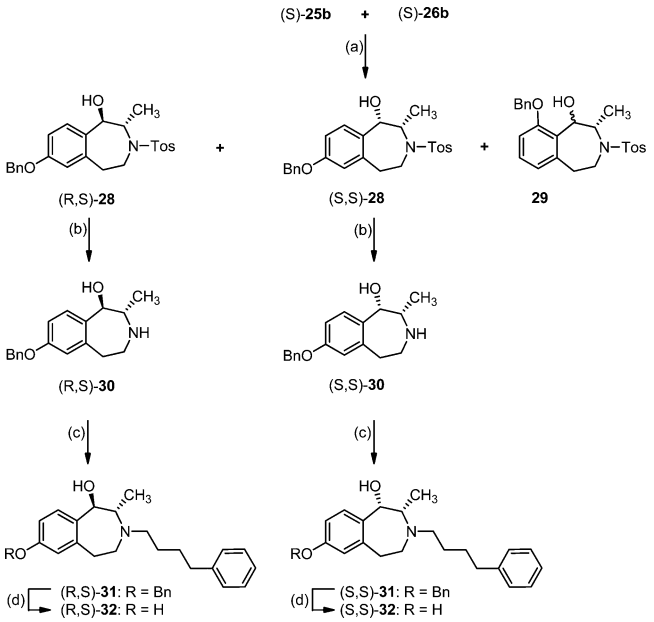

[a]Reagents and reaction conditions: (a) $NaBH_4$, CH_3OH, 20 h, rt. (b) Mg, CH_3OH, Δ, 36 h. (c) 1-Chloro-4-phenylbutane, CH_3CN, K_2CO_3, Bu_4NI, Δ, 72 h. (d) H_2, Pd/C, 1 bar, CH_3OH, 1 h, rt. The enantiomers (*S*,*R*)-**31**, (*S*,*R*)-**32**, (*R*,*R*)-**31**, and (*R*,*R*)-**32** were prepared in the same manner starting with (*R*)-**25b** and (*R*)-**26b**.

(*S*,*S*)-**28** was performed with magnesium in methanol, providing the secondary amines (*R*,*S*)-**30** and (*S*,*S*)-**30** in 65% and 60% yields, respectively, which were alkylated subsequently with 1-chloro-4-phenylbutane to yield the tertiary amines (*R*,*S*)-**31** and (*S*,*S*)-**31**. The corresponding enantiomers (*S*,*R*)-**31** and (*R*,*R*)-**31** were synthesized analogously starting with (*R*)-alanine ((*R*)-**11**).

Analysis of the enantiomeric purity of the stereoisomeric benzyl ethers **31** showed considerable racemization (Table SI-3). Therefore, the phenylbutylamines **31** were purified by chiral HPLC (Chiralpak AD) to obtain the stereoisomeric phenylbutyl substituted 3-benzazepines (*R*,*S*)-**31**, (*S*,*S*)-**31**, (*S*,*R*)-**31**, and (*R*,*R*)-**31** with high enantiomeric excess (98.4−100% ee) (Table SI-3, Figure SI-2A−D). The configuration of the stereoisomers **31** was derived from the configuration of the analogous stereoisomeric methyl ethers **21**. However, an X-ray crystal structure analysis of the mixture of (*S*,*R*)-**28**/(*R*,*S*)-**28**[24] confirmed unequivocally the *trans*-configuration and thus the relative and absolute configuration of all four stereoisomers of **28** and **31** (Figure SI-6).

Finally the benzyl protective group of the stereoisomeric benzyl ethers **31** was removed hydrogenolytically with H_2 and Pd/C. The enantiomers (*S*,*S*)-**31** and (*R*,*R*)-**31** were thus converted into the phenols (*S*,*S*)-**32**, and (*R*,*R*)-**32**, respectively. The enantiomerically pure phenols (*R*,*S*)-**32** and (*S*,*R*)-**32** were obtained by hydrogenolytic cleavage of the racemic mixture (*S*,*R*)-**31**/(*R*,*S*)-**31** and subsequent separation of the enantiomers by chiral preparative HPLC (Figure SI-3).

RECEPTOR AFFINITY

Affinity toward GluN2B Containing NMDA Receptors. The affinity toward GluN2B containing NMDA receptors of the stereoisomeric 2-methyl-3-benzazepin-1-ols **21**, **31**, and **32** was determined in a competitive receptor binding assay, which was recently developed in our group.[25] Membrane preparations obtained by ultrasonic irradiation of L(tk−) cells stably expressing recombinant human GluN1a and GluN2B subunits forming functional NMDA receptors were used as receptor material, and tritium labeled [^{3}H]**1** served as radioligand. The high amount of GluN2B containing NMDA receptors renders this system selective, despite the limited selectivity of the radioligand. After the adherent growing cells reached approximately 90% confluency, dexamethasone was added to the growth medium to induce the synthesis of NMDA receptors. During this period, cell death was inhibited by addition of the NMDA receptor antagonist ketamine interacting with the phencyclidine binding site within the channel pore.[25,26]

The affinity toward GluN2B containing NMDA receptors is summarized in Table 1. The GluN2B affinity of the phenols **32** is generally slightly higher than the GluN2B affinity of the methyl ethers **21**, but they show the same relationship between the stereochemistry and the GluN2B affinity. The affinity increases in the following order: (1*R*,2*S*) < (1*S*,2*S*) < (1*S*,2*R*) < (1*R*,2*R*). In both series the (*R*,*R*)-configured stereoisomers show the highest GluN2B affinity of 17 nM ((*R*,*R*)-**32**) and 41 nM ((*R*,*R*)-**21**). Whereas the GluN2B affinity of the (*R*,*S*)-configured stereoisomers (*R*,*S*)-**21** and (*R*,*S*)-**32** is considerably reduced, the GluN2B affinity of the other three stereoisomers is in a similar range, respectively.

The lead compounds **1** and **2** have (*S*)-configuration at both centers of chirality. The corresponding (*S*,*S*)-configured stereoisomers (*S*,*S*)-**21** and (*S*,*S*)-**32** display slightly reduced GluN2B affinity compared with the (*R*,*R*)- and (*S*,*R*)-configured stereoisomers. However, taking the SEM values into account, the differences between the (*S*,*S*)-, (*R*,*R*)-, and (*S*,*R*)-configured stereoisomers are very small. Nevertheless the low stereoselectivity in the interaction with GluN2B receptors was unexpected.

Moreover the high GluN2B affinity of the stereoisomeric benzyl ethers **31**, originally prepared as synthetic intermediates, was very surprising. In general the GluN2B affinity of the benzyl ethers **31** exceeds the GluN2B affinity of the methyl ethers **21** and the phenols **32** (exception (*S*,*R*)-**32**). The most potent stereoisomer (*R*,*S*)-**31** reveals a K_i value of 9.3 nM, which is even lower than the K_i values of the reference compounds **1** and eliprodil.

In all three series of 3-benzazepines, **21**, **31**, and **32**, the additional methyl moiety has a considerable influence on the GluN2B affinity. In cases of the phenols **32** and the methyl ether **21** the additional methyl moiety leads to a slight reduction of the GluN2B affinity compared to **5** and **6**. On the contrary the GluN2B affinity of the benzyl ethers **31** was dramatically increased upon introduction of the methyl moiety in 2-position, which can be seen by comparing the K_i values of **7** and **31** stereoisomers.

Receptor Selectivity. In addition to the affinity toward the ifenprodil binding site of the NMDA receptor, the affinities toward the phencyclidine binding site of the NMDA receptor[27,28] and the affinity toward σ_1 and σ_2 receptors[29−31] were recorded in receptor binding studies (Table 1). In general

DOI: 10.1021/acs.jmedchem.5b00897
J. Med. Chem. XXXX, XXX, XXX−XXX

Table 1. Affinities of 2-Methyl-3-benzazepin-1-ols to the Ifenprodil Binding Site of GluN2B Containing NMDA Receptors, the PCP Binding Site of the NMDA Receptor and to σ_1 and σ_2 Receptors[a]

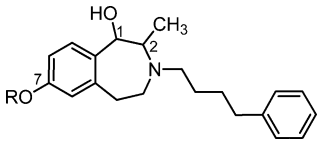

			K_i ± SEM (nM)				
compd	R	configuration	GluN2B	PCP	σ_1	σ_2	ΔH (kcal/mol) (MM/GBSA)
5[17]	H	*rac*	14 ± 1.5	35%	194	>10 μM	
6[16]	CH_3	*rac*	5.4 ± 0.4	22%	182	554	
7[17]	Bn	*rac*	187 ± 72	39%	293	>1 μM	
(*S*,*S*)-**21**	CH_3	1*S*,2*S*	67 ± 16	47%[b]	4.5 ± 0.5	25 ± 2.7	−50.65 ± 3.80
(*R*,*R*)-**21**	CH_3	1*R*,2*R*	41 ± 0.7	28%[b]	3.2 ± 0.8	19 ± 2.4	−54.37 ± 3.30
(*S*,*R*)-**21**	CH_3	1*S*,2*R*	47 ± 9.4	29%[b]	6.3 ± 2.0	48 ± 9.0	−49.89 ± 3.05
(*R*,*S*)-**21**	CH_3	1*R*,2*S*	224 ± 22	33%[b]	42 ± 5.7	6.1 ± 0.9	−45.79 ± 4.20
(*S*,*S*)-**31**	Bn	1*S*,2*S*	28 ± 3.1	0%[b]	196	826	−58.10 ± 3.70
(*R*,*R*)-**31**	Bn	1*R*,2*R*	14 ± 3.5	17%[b]	13 ± 2.0	138	−60.45 ± 3.40
(*S*,*R*)-**31**	Bn	1*S*,2*R*	38 ± 7.8	47%[b]	46 ± 13	154	−53.94 ± 2.90
(*R*,*S*)-**31**	Bn	1*R*,2*S*	9.3 ± 0.4	48%[b]	31 ± 5.2	44 ± 18	−64.12 ± 2.99
(*S*,*S*)-**32**	H	1*S*,2*S*	31 ± 13	1440	326 ± 36	129 ± 26	−61.12 ± 2.80
(*R*,*R*)-**32**	H	1*R*,2*R*	17 ± 5.7	37%[b]	86 ± 2.5	148 ± 11	−53.46 ± 3.19
(*S*,*R*)-**32**	H	1*S*,2*R*	26 ± 11	39%[b]	665 ± 96	66 ± 6.9	−54.28 ± 2.67
(*R*,*S*)-**32**	H	1*R*,2*S*	180 ± 52	9%[b]	56 ± 7.7	129 ± 26	−49.62 ± 2.12
1			10 ± 0.7		125 ± 24	98.3 ± 34	
eliprodil			13 ± 2.5				
dexoxadrol				32 ± 7.4			
haloperidol					6.3 ± 1.6	78.1 ± 2.3	
di-*o*-tolylguanidine					89 ± 29	57.5 ± 18	

[a]The right column gives the binding energy ΔH (kcal/mol) calculated using the MM/GBSA method. [b]For low-affinity compounds only the inhibition of the radioligand binding at a test compound concentration of 1 μM is given.

Table 2. Inhibition of NMDA Receptor Mediated Excitotoxicity by 2-Methyl-3-benzazepin-1-ols 21, 31, and 32 Using Cell Lines Stably Expressing GluN2B and GluN2A Subunit Containing NMDA Receptors, Respectively[a]

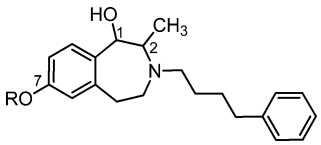

compd	R	config	K_i ± SEM (nM) GluN2B affinity	excitotox (%)[b] (GluN2B)	IC_{50} ± SEM (nM) GluN2B activity	excitotox (%)[c] (GluN2A)
5[17]	H	*rac*	14 ± 1.5		18.6 ± 9.8	>90
6[16]	CH_3	*rac*	5.4 ± 0.4		360 ± 6.5	>90
7[17]	Bn	*rac*	187 ± 72			
(*S*,*S*)-**21**	CH_3	1*S*,2*S*	67 ± 16	−1.1 ± 3.6	650 ± 41	132 ± 36
(*R*,*R*)-**21**	CH_3	1*R*,2*R*	41 ± 0.7	86 ± 2	nd	114 ± 10
(*S*,*R*)-**21**	CH_3	1*S*,2*R*	47 ± 9.4	12 ± 3.4	5850 ± 2200	114 ± 16
(*R*,*S*)-**21**	CH_3	1*R*,2*S*	224 ± 22	4.4 ± 5.7	119 ± 15	106 ± 2.7
(*S*,*S*)-**31**	Bn	1*S*,2*S*	28 ± 3.1	50 ± 9.0	nd	177 ± 89
(*R*,*R*)-**31**	Bn	1*R*,2*R*	14 ± 3.5	118 ± 3.3	nd	366 ± 186
(*S*,*R*)-**31**	Bn	1*S*,2*R*	38 ± 7.8	41 ± 12	nd	102 ± 18
(*R*,*S*)-**31**	Bn	1*R*,2*S*	9.3 ± 0.4	24 ± 6.7	5600 ± 1500	116 ± 18
(*S*,*S*)-**32**	H	1*S*,2*S*	31 ± 13	7.6 ± 4.3	167 ± 33	46 ± 10
(*R*,*R*)-**32**	H	1*R*,2*R*	17 ± 5.7	1.4 ± 2.3	41 ± 14	81 ± 8
(*S*,*R*)-**32**	H	1*S*,2*R*	26 ± 11	4.1 ± 2.4	9.0 ± 1.9	91 ± 9.4
(*R*,*S*)-**32**	H	1*R*,2*S*	180 ± 52	1.2 ± 1.9	225 ± 34	87 ± 9
memantine				51.9 ± 19.8	5323 ± 1238	50.0 ± 14.3

[a]excitotox = excitotoxicity; inhib = inhibition; nd = not determined. [b]Cytotoxicity after addition of 10 μM test compound, (*S*)-glutamate, and glycine to GluN2B producing L13-E6 cells; IC_{50} values were determined only when the excitotoxicity in the screening was below 40% of controls. [c]Cytotoxicity after addition of 10 μM test compound, (*S*)-glutamate, and glycine to GluN2A producing L12-G10 cells.

DOI: 10.1021/acs.jmedchem.5b00897
J. Med. Chem. XXXX, XXX, XXX−XXX

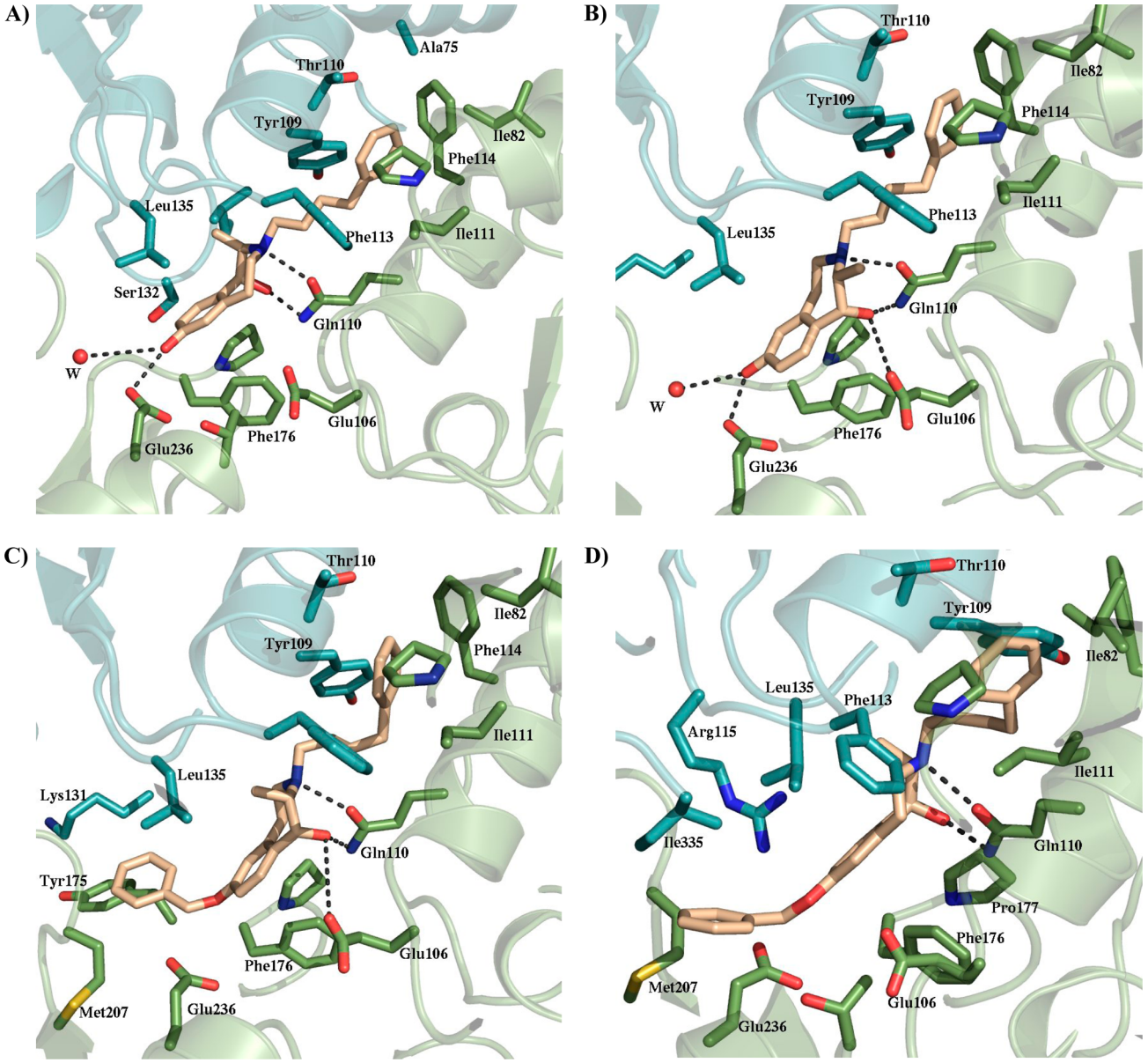

Figure 3. (A) Binding mode of (*S*,*R*)-**32** (beige). GluN1b residues are colored in cyan and GluN2B in green. H-bonds are shown as black dashed lines. (B) Binding mode of (*R*,*R*)-**32** (beige). GluN1b residues are colored in cyan and GluN2B in green. H-bonds are shown as black dashed lines. (C) Binding mode of (*R*,*S*)-**31** (beige). GluN1b residues are colored in cyan and GluN2B in green. H-bonds are shown as black dashed lines. (D) Binding mode of (*S*,*S*)-**31** (beige). GluN1b residues are colored in cyan and GluN2B in green. H-bonds are shown as black dashed lines.

the affinity toward the phencyclidine binding site of all compounds is rather low, indicating high selectivity of the 3-benzazepines **21**, **31**, and **32** toward the ifenprodil binding site over the phencyclidine binding site.

The phenols **32** reveal moderate σ_1 and σ_2 affinity leading at least for the high affinity GluN2B ligands (*S*,*S*)-**32**, (*R*,*R*)-**32**, and (*S*,*R*)-**32** to considerable selectivity over the σ receptors. However, some of the methyl ethers **21** represent very potent σ_1 and/or σ_2 ligands as well. The σ_1 affinity of (*S*,*S*)-**21**, (*R*,*R*)-**21**, and (*S*,*R*)-**21** is in the low nanomolar range indicating even a preference for the σ_1 receptor over the GluN2B receptor. Additionally the least potent GluN2B stereoisomer (*R*,*S*)-**21** ($K_i(\sigma_2)$ = 6.1 nM) represents a potent and selective σ_2 ligand.

In the case of the benzyl ethers **31** the stereochemistry has a strong impact on receptor selectivity. The most potent GluN2B ligand (*R*,*S*)-**31** has a 3-fold selectivity over the σ_1 receptor and a 4-fold selectivity over the σ_2 subtype. The next potent GluN2B ligand (*R*,*R*)-**31** reveals the same affinity toward the ifenprodil binding site and the σ_1 receptor but a 10-fold preference over the σ_2 receptor. The stereoisomer (*S*,*R*)-**31** shows a similar binding profile at the three receptors as (*R*,*R*)-**31**. The highest selectivity for GluN2B receptors over σ_1 (7-fold) and σ_2 receptors (30-fold) was observed for the stereoisomer (*S*,*S*)-**31**.

FUNCTIONAL ACTIVITY

The functional activity of the stereoisomeric 3-benzazepines **21**, **31**, and **32** was determined in excitotoxicity assays. For this purpose L(tk−) cell lines L13-E6 and L12-G10 stably expressing GluN1a/GluN2B and GluN1a/GluN2A subunits, respectively, were grown and stimulated by dexamethasone to produce the corresponding NMDA receptor subunits. Thirty

DOI: 10.1021/acs.jmedchem.5b00897
J. Med. Chem. XXXX, XXX, XXX−XXX

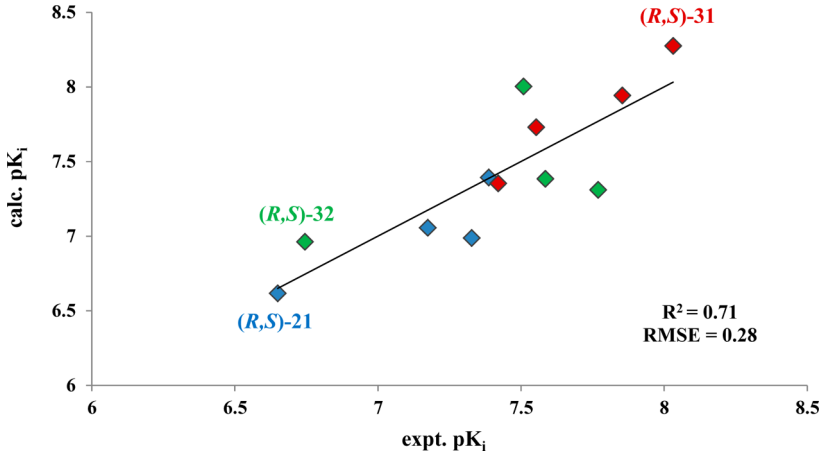

Figure 4. Correlation between calculated pK_i values (calc pK_i) and experimentally determined pK_i values (expt pK_i) (**21** blue points, **31** red points, **32** green points). The binding energy was calculated by MM/GBSA method, and the calc pK_i values were obtained from the linear regression equation ($\Delta H = -11.05\ pK_i + 27.317$).

minutes after addition of different amounts of a test compound, the excitotoxicity induced by (*S*)-glutamate and glycine was recorded by determination of the released amount of lactate dehydrogenase (LDH).[32] Experiments using L13-E6 and L12-G10 cell lines show the effects on GluN2B and GluN2A containing NMDA receptors, respectively.

In Table 2 the effects of the stereoisomeric 3-benzaepines **21**, **31**, and **32** on the glutamate/glycine induced cytotoxicity toward GluN2B and GluN2A producing cells are summarized and correlated with the GluN2B affinity and stereochemistry.

Although the benzyl ethers **31** display high GluN2B affinity (K_i = 9−38 nM), they are not able to inhibit the glutamate/glycine induced excitotoxicity at the screening concentration of 10 μM. Only the highly affine ligand (*R*,*S*)-**31** (K_i = 9.3 nM) reduced the cytotoxicity (GluN2B cells) considerably (23% of controls), but recording the exact dose−response curves resulted in an IC_{50} value greater than 5 μM.

The stereoisomeric methyl ethers **21** reveal the lowest GluN2B affinity (K_i = 41−224 nM) of this series of compounds. With the exception of the (*R*,*R*)-configured stereoisomer (*R*,*R*)-**21**, the cytotoxic effects of glutamate and glycine were reduced in the screening at a concentration of 10 μM. Finally the highest cytoprotective activity was found for the (*R*,*S*)-configured stereoisomer (*R*,*S*)-**21** with an IC_{50} value of 119 nM.

The phenols **32** represent the most promising group within this series of GluN2B ligands. At a concentration of 10 μM all four stereoisomers **32** displayed high cytoprotective effects. The resulting IC_{50} values correlate nicely with the K_i values describing binding at the GluN2B receptor. The (*R*,*R*)- and (*S*,*R*)-configured ligands (*R*,*R*)-**32** and (*S*,*R*)-**32** reveal the highest GluN2B affinity (K_i = 17 and 26 nM) and the highest inhibition of excitotoxicity of GluN2B subunit producing cells (IC_{50} = 41 and 9 nM). For the judgment of the affinity data of (*R*,*R*)-**32** and (*S*,*R*)-**32** the high SEM values have to be taken into account. The strong protection of GluN2B subunit producing cells by (*S*,*R*)-**32** (IC_{50} = 9.0 nM) indicates strong allosteric NMDA receptor antagonism.

At a test compound concentration of 10 μM the stereoisomeric 3-benzazepines **21**, **31**, and **32** could not inhibit the glutamate/glycine induced cytotoxic effects on GluN2A subunit containing cells. Obviously the 3-benzazepines represent GluN2B selective NMDA receptor antagonists, which do not inhibit GluN2A containing NMDA receptors.

MOLECULAR MODELING STUDIES

In order to analyze the binding mode of the tetrahydro-3-benzazepines **21**, **31**, and **32** and study the effect of their respective configuration on the binding to NMDA receptors, the different stereoisomers were docked into the binding pocket formed by the dimer of the N-terminal domains of GluN1b and GluN2B subunits of the NMDA receptor. The obtained binding modes were further assessed by molecular dynamic (MD) studies coupled with MM/GBSA binding energy calculations.

Our docking studies showed that all the herein reported tetrahydro-3-benzazepine derivatives adopt a similar binding mode as found with **1** (Figure SI-7). Generally, the phenyl group attached at the end of the butyl linker is embedded in the same hydrophobic region as the benzyl group of **1** and is stabilized by a cluster of hydrophobic amino acid residues in GluN1 (Tyr109 and Ala75) and GluN2B (Pro78, Ile111, and Phe114). The aromatic ring of the benzazepine moiety overlaps with the corresponding phenolic group in **1**, where it undergoes similar hydrophobic interactions with Leu135 (GluN1), Phe176 and Pro177 (GluN2B). Similar to the piperidine-N of **1**, the protonated benzazepine-N is able to form an H-bond with the amide-oxygen of Gln110 side chain (GluN2B), whereas the hydroxy group establishes H-bond interaction with the amide-NH of Gln110 (GluN2B) or with the carboxylate group of Glu106 (GluN2B).

The phenols **32** form H-bond interaction with Glu236 (GluN2B) like **1** (Figure 3A,B), which is lost with the methyl and benzyl ethers **21** and **31**. However, the additional benzyl moiety in **31** protrudes into an adjacent subpocket which explains the unexpected high affinity. In the cases of (*R*,*S*)-**31** (Figure 3C) and (*R*,*R*)-**31** the benzyl group is surrounded by hydrophobic residues, namely, Leu135 (GluN1b), Tyr175 (GluN2B), and Met207 (GluN2B), whereas the benzyl group of (*S*,*S*)-**31** (Figure 3D) and (*S*,*R*)-**31** interacts with Ile335 (GluN1b), Met207 (GluN2B) with the possibility of undergoing a cation−π interaction with Arg115 in GluN1b.

The effect of the configuration at 1- and 2-position seems to be mainly reflected in the positioning of both substituents in the binding pocket. The 1-hydroxy and 2-methyl substituents in

DOI: 10.1021/acs.jmedchem.5b00897
J. Med. Chem. XXXX, XXX, XXX−XXX

the (1*S*,2*R*)- and (1*S*,2*S*)-configured stereoisomers show an overlap with the hydroxy and methyl groups in **1** (Figure 3A,D and Figure SI-7). There, the hydroxy group establishes an H-bond with the amide-NH of Gln110. In the (1*R*,2*R*)- and (1*R*,2*S*)-configured stereoisomers, the benzazepine scaffold is flipped by 180° and both substituents are sitting in opposite direction to the substituents in **1**, moving closer to the GluN2B chain (Figure 3B and Figure 3C). This allows the 1-hydroxy group to form an additional H-bond with the side chain of Glu106 (GluN2B) in addition to the H-bond formed with the amide-NH of Gln110. The postulated binding modes of selected representatives for each configuration are depicted in Figure 3 and the binding modes of the other derivatives are shown in Figure SI-8.

All the suggested binding modes were stable during the 10 ns MD simulation as shown by the rmsd plots (Figure SI9A–L). They showed favorable binding energies (Table 1), calculated by the MM/GBSA method, and the established H-bonds were maintained throughout the MD simulation. (Figure SI-9)

A significant correlation between the estimated binding energies (MM/GBSA) and the observed affinities for GluN2B containing NMDA receptors was obtained (Table 1, Figure 4). Even when the correlation is not perfect, some useful observations can be made. Most importantly, the (*R*,*S*)-configured phenol and methyl ether (*R*,*S*)-**21** and (*R*,*S*)-**32** show the least favorable binding energies among all tested compounds, which is in line with their reduced affinities for the GluN2B containing NMDA receptors. (*R*,*S*)-**31**, which displayed the highest affinity among the benzyl ethers **31** and exhibited higher potency than all the herein tested compounds, showed the most favorable binding energy.

CONCLUSION

Three sets of stereoisomeric 2-methyltetrahydro-3-benzazepin-1-ols were prepared, evaluated in receptor binding studies and functional activity assays, and finally docked into the ifenprodil binding site of the cocrystallized GluN1b/GluN2B dimer. The binding modes of the differently substituted and configured compounds were analyzed and evaluated by MM/GBSA method. According to this analysis, the phenols **32** form a similar H-bond with Glu236 (GluN2B) as the phenol of **1**. A flip of 180° of the 3-benzazepine scaffold explains the similar GluN2B affinity of the stereoisomeric phenols (*S*,*S*)-**32**, (*R*,*R*)-**32**, and (*S*,*R*)-**32** and methyl ethers of (*S*,*S*)-**21**, (*R*,*R*)-**21**, and (*S*,*R*)-**21**. The reversed binding modes are responsible for the low influence of the ligand configuration on the GluN2B binding affinity. This result will be taken into account during the design and development of novel GluN2B selective NMDA antagonists.

The receptor binding studies showed unexpectedly high GluN2B affinity of the benzyl ethers **31**, which even exceeds the GluN2B affinity of the phenols **32**. Analysis of the docking experiments resulted in an additional hydrophobic subpocket formed by lipophilic residues of different amino acids of both subunits (e.g., Leu135 (GluN1b), Ile335 (GluN1b), Tyr175 (GluN2B), Met207 (GluN2B)). This so far undetected lipophilic subpocket of the GluN1b/GluN2B dimer will be further exploited by modification of the lipophilic benzyl residue of the ligands with the aim to find potent and selective modulators of the NMDA receptor.

In functional assays the cytoprotective effects of the phenols **32** correlate nicely with their GluN2B affinity. The most promising ligands of this series are the (*R*,*R*)- and (*S*,*R*)-configured phenols (*R*,*R*)-**32** and (*S*,*R*)-**32** with high GluN2B affinity (K_i = 17 nM and K_i = 26 nM) and strong cytoprotective effects (IC_{50} = 41 nM and IC_{50} = 9 nM). However, the benzyl ethers **21** did not show cytoprotective effects in the functional assays despite their high GluN2B binding affinity (K_i = 9–38 nM). It was shown that the benzyl ethers **21** are able to open a lipophilic subpocket close to the ifenprodil binding site resulting in high GluN2B affinity. However, these interactions are not able to induce the conformational changes of the receptor protein, which are required to close the ion channel.

EXPERIMENTAL SECTION

Chemistry. General. Thin layer chromatography (tlc): silica gel 60 F254 plates (Merck). Flash chromatography (fc): silica gel 60, 40–64 μm (Merck); parentheses include diameter of the column, eluent, fraction size, R_f value. Melting point: melting point apparatus SMP 3 (Stuart Scientific), uncorrected. Optical rotation: polarimeter 341 (PerkinElmer), wavelength 589 nm, path length (*l*), 1 dm; +20 °C; unit [deg mL dm^{-1} g^{-1}] is omitted, concentration [mg/mL] and solvent given in parentheses. ^{1}H NMR (400 MHz): Unity Mercury Plus 400 spectrometer (Varian); δ in ppm related to tetramethylsilane; coupling constants are given with 0.5 Hz resolution. The purity of all described compounds including the test compounds is greater than 95%. For compound **10** and the four stereoisomers of **20** an elemental analysis was performed. The purity of all other compounds was analyzed by HPLC.

Methyl (*S*)-2-{*N*-[2-(3-Methoxyphenyl)ethyl]-*N*-(4-tosyl)-amino}propionate ((*S*)-13). Under N_2, sulfonamide (*S*)-**12** (7.74 g, 50 mmol) was dissolved in absolute THF (600 mL) and cooled to 0 °C. Then phenylethanol **10** (13.1 g, 50 mmol), Ph_3P (40.3 g, 0.15 mol), and DIAD (29.7 mL, 0.15 mol) were added dropwise. The mixture was stirred at 0 °C for 1 h and at rt for 16 h. Then the solution was diluted with *n*-hexane (700 mL) and the precipitated $Ph_3P{=}O$ was removed by filtration. The solvent was evaporated in vacuum and the residue was purified by fc (8 cm, *n*-hexane/ethyl acetate 8:2, 65 mL, R_f = 0.35). Colorless oil, yield (13.9 g, 71%). $[\alpha]_D$ −53.7 (*c* 1.15, CH_3OH). $C_{20}H_{25}NO_5S$ (391.3). ^{1}H NMR ($CDCl_3$): δ (ppm) = 1.36 (d, *J* = 7.3 Hz, 3H, N-CH-CH_3), 2.39 (s, 3H, Ph-CH_3), 2.81–2.91 (m, 1H, Ph-CH_2-CH_2-N), 2.96–3.05 (m, 1H, Ph-CH_2-CH_2-N), 3.21–3.31 (m, 1H, Ph-CH_2-CH_2-N), 3.43–3.49 (m, 1H, Ph-CH_2-CH_2-N), 3.47 (s, 3H, CO_2-CH_3), 3.78 (s, 3H, OCH_3), 4.64 (q, *J* = 7.3 Hz, 1H, N-C*H*-CH_3), 6.71–6.77 (m, 3H, 2-H phenyl, 4-H phenyl, 6-H phenyl), 7.19 (t, *J* = 7.7 Hz, 1H, 5-H phenyl), 7.25 (d, *J* = 8.6 Hz, 2H, 3-H tosyl and 5-H tosyl), 7.69 (d, *J* = 8.4 Hz, 2H, 2-H tosyl and 6-H tosyl).

(*S*)-2-{*N*-[2-(3-Methoxyphenyl)ethyl]-*N*-(4-tosyl)amino}-propionic Acid ((*S*)-14). (*S*)-**13** (1.54 g, 3.95 mmol) was dissolved in a THF/H_2O mixture (7:3, 60 mL), and LiOH·H_2O (1.26 g, 19.8 mmol) was added. The mixture was stirred for 24 h at rt. Then the mixture was neutralized with 6 M HCl and the aqueous layer was extracted with diethyl ether (4 × 30 mL). The combined organic layers were dried (Na_2SO_4), the solvent was evaporated in vacuum, and the residue was purified by fc (2 cm, *n*-hexane/ethyl acetate 2:8, 30 mL, R_f = 0.35). Colorless oil, yield 1.63 g (87%). $[\alpha]_D$ −22.0 (*c* 1.06, CH_3OH). $C_{19}H_{23}NO_5S$ (377.4). ^{1}H NMR ($CDCl_3$): δ (ppm) = 1.36 (d, *J* = 7.2 Hz, 3H, N-CH-CH_3), 2.39 (s, 3H, Ph-CH_3), 2.80–2.87 (m, 1H, Ph-CH_2-CH_2-N), 2.93–3.00 (m, 1H, Ph-CH_2-CH_2-N), 3.25–3.33 (m, 1H, Ph-CH_2-CH_2-N), 3.39–3.47 (m, 1H, Ph-CH_2-CH_2-N), 3.75 (s, 3H, OCH_3), 4.57 (q, *J* = 7.1 Hz, 1H, N-C*H*-CH_3), 6.67–6.68 (m, 1H, 2-H phenyl), 6.71–6.74 (m, 2H, 4-H, 6-H phenyl), 7.16 (t, *J* = 7.9 Hz, 1H, 5-H phenyl), 7.23 (d, *J* = 8.0 Hz, 2H, 3-H tosyl and 5-H tosyl), 7.69 (d, *J* = 8.3 Hz, 2H, 2-H tosyl and 6-H tosyl). A signal for the CO_2H proton is not visible in the spectrum.

(*S*)-7-Methoxy-2-methyl-3-(*p*-tosyl)-2,3,4,5-tetrahydro-3-benzazepin-1-one ((*S*)-15), (*S*)-9-Methoxy-2-methyl-3-(*p*-tosyl)-2,3,4,5-tetrahydro-3-benzazepin-1-one ((*S*)-16), 6-Methoxy-1-methyl-2-(*p*-tosyl)-1,2,3,4-tetrahydroisoquinoline (17a), and 8-Methoxy-1-methyl-2-(*p*-tosyl)-1,2,3,4-tetrahydroisoquinoline (17b). Under N_2 the acid (*S*)-**14** (5.10 g, 14.0 mmol) was dissolved in CH_2Cl_2 (300 mL) and the solution was cooled to −30 °C. Then

DOI: 10.1021/acs.jmedchem.5b00897
J. Med. Chem. XXXX, XXX, XXX−XXX

trifluoroacetic acid anhydride (9.56 mL, 68.0 mmol) was added and the mixture was stirred for 1 h at −30 °C. Afterward, $SnCl_4$ (6.55 mL, 56.0 mmol) was added slowly. After 22 h of stirring at −30 °C, the solution was neutralized with 5 M NaOH at 0 °C and the aqueous layer was extracted with CH_2Cl_2 (3 × 50 mL). The organic layer was dried (Na_2SO_4), concentrated in vacuum, and the residue was purified by fc (8 cm, *n*-hexane/ethyl acetate 7:3, 65 mL, R_f (**17**) = 0.68) and R_f ((*S*)-**15** and (*S*)-**16**) = 0.36).

17a and **17b** (R_f = 0.68): Pale yellow solid, mp 96 °C, yield 0.79 g (17%).

(*S*)-**15** and (*S*)-**16** (R_f = 0.36): Colorless solid, yield 2.94 g (59%).

Spectroscopic data of the mixtures (*S*)-**15**/(*S*)-**16**: $C_{19}H_{21}NO_4S$ (359.2). ^{1}H NMR (CD_3OD): δ (ppm) = 1.44 (d, J = 7.5 Hz, 3 × 0.5H, N-CH-CH_3), 1.46 (d, J = 7.2 Hz, 3 × 0.5H, N-CH-CH_3), 2.34 (s, 3 × 0.5H, Ph-CH_3), 2.35 (s, 3 × 0.5H, Ph-CH_3), 2.72−2.84 (m, 3 × 0.5H, 5-H), 2.91−3.02 (m, 0.5H, 5-H), 3.45−3.52 (m, 2 × 0.5H, 2 × 4-H), 3.66 (s, 3 × 0.5H, OCH_3), 3.81 (s, 3 × 0.5H, OCH_3), 3.84−3.92 (m, 0.5H, 4-H), 3.94−4.05 (m, 0.5H, 4-H), 4.71 (q, J = 7.1 Hz, 0.5H, 2-H), 4.77 (q, J = 7.8 Hz, 0.5H, 2-H), 6.54 (d, J = 2.5 Hz, 0.5H, 6-H●), 6.64 (d, J = 7.4 Hz, 0.5H, 6-H□), 6.69 (dd, J = 8.5/2.5 Hz, 0.5H, 8-H●), 6.70 (d, J = 8.4 Hz, 0.5H, 8-H□), 7.04 (br d, J = 8.0 Hz, 2 × 0.5H, 3-H tosyl and 5-H tosyl), 7.06 (d, J = 8.0 Hz, 2 × 0.5H, 3-H tosyl and 5-H tosyl), 7.31 (d, J = 8.5 Hz, 0.5H, 9-H●), 7.21−7.25 (m, 0.5H, 7-H□), 7.30 (br d, J = 8.3 Hz, 2 × 0.5H, 2-H tosyl and 6-H tosyl).7.35 (d, J = 8.3 Hz, 2 × 0.5H, 2-H tosyl and 6-H tosyl). The ratio of regioisomers **15** (marked with ●)/**16** (marked with □) is 50:50.

(1*R*,2*S*)-7-Methoxy-2-methyl-2,3,4,5-tetrahydro-1*H*-3-benzazepin-1-ol ((*R*,*S*)-20). Sulfonamide (*R*,*S*)-**18** (0.72 g, 2.17 mmol) was dissolved in CH_3OH (85 mL), and Mg (1.13 g, 47.2 mmol) was added. The reaction mixture was heated to reflux for 18 h. 2 M HCl was added, residual Mg was filtered off, the pH value was adjusted to pH 9−10 by addition of 2 M NaOH, and the aqueous layer was extracted with CH_2Cl_2 (5 × 40 mL). The organic layer was dried (Na_2SO_4), concentrated in vacuum, and the residue was purified by fc (4 cm, ethyl acetate/CH_3OH 95:5 + 2% *N*,*N*-dimethylethanamine, 30 mL, R_f = 0.07). Pale yellow oil, yield 254 mg (57%). $[\alpha]_D$ +0.13 (*c* 0.99, CH_3OH, 34% ee). $C_{12}H_{17}NO_2$ (207.3). ^{1}H NMR ($CDCl_3$): δ (ppm) = 0.93 (d, J = 6.9 Hz, 3H, N-CH-CH_3), 2.42 (br s, 1H, NH), 2.54 (ddd, J = 14.9/5.4/1.6 Hz, 1H, 5-H), 2.91 (ddd, J = 13.4/5.4/2.9 Hz, 1H, 4-H), 3.00−3.06 (m, 1H, 5-H), 3.27−3.36 (m, 2H, 2-H and 4-H), 3.76 (s, 3H, OCH_3), 4.36 (d, J = 5.4 Hz, 1H, 1-H), 6.61 (br s, 1H, 6-H), 6.62 (dd, J = 8.8/2.7 Hz, 1H, 8-H), 7.04 (d, J = 8.8 Hz, 1H, 9-H). A signal for the OH proton is not visible.

(1*R*,2*S*)-7-Methoxy-2-methyl-3-(4-phenylbutyl)-2,3,4,5-tetrahydro-1*H*-3-benzazepin-1-ol ((*R*,*S*)-21) and (1*S*,2*R*)-7-Methoxy-2-methyl-3-(4-phenylbutyl)-2,3,4,5-tetrahydro-1*H*-3-benzazepin-1-ol ((*S*,*R*)-21). A mixture of the secondary amine (*R*,*S*)-**20** (70.8 mg, 0.34 mmol), 1-chloro-4-phenylbutane (111.4 μL, 0.68 mmol), TBAI (251.2 mg, 0.68 mmol), K_2CO_3 (188.0 mg, 1.36 mmol), and CH_3CN (10 mL) was heated to reflux for 72 h. The mixture was filtered, and the filtrate was concentrated in vacuum. The residue was purified by fc (2 cm, *n*-hexane/ethyl acetate 95:5 and 1% *N*,*N*-dimethylethanamine, 10 mL, R_f = 0.10) to afford a mixture of the enantiomers (*R*,*S*)-**21** and (*S*,*R*)-**21**, in the ratio of 67:33. Colorless solid, mp 113 °C, yield 55.6 mg (48%). Purity (HPLC): 98.1%, t_R = 18.7 min. The enantiomers (*R*,*S*)-**21** and (*S*,*R*)-**21** were separated on an analytical chiral HPLC (column, Chiralpak AD (Chiral Technologies Europe), solvent *n*-hexane/isopropanol (9:1), t_R ((*R*,*S*)-**21**) = 11.5 min, t_R ((*S*,*R*)-**21**) = 14.4 min). (*R*,*S*)-**21**: Colorless oil. $[\alpha]_D$ +31.8 (*c* 0.53, CH_3OH, 99.8% ee). (*S*,*R*)-**21**: Colorless resin. $[\alpha]_D$ −32.4 (*c* 0.52, CH_3OH, 99.4% ee). Spectroscopic data of (*R*,*S*)-**21** and (*S*,*R*)-**21**: $C_{22}H_{29}NO_2$ (339.5). ^{1}H NMR ($CDCl_3$): δ (ppm) = 0.64 (d, J = 6.8 Hz, 3H, N-CH-CH_3), 1.52−1.62 (m, 2H, N-CH_2-CH_2-CH_2-CH_2-Ph), 1.64−1.73 (m, 2H, N-CH_2-CH_2-CH_2-CH_2-Ph), 2.49 (ddd, J = 10.9/4.9/1.5 Hz, 1H, 5-H), 2.52 (t, J = 7.1 Hz, 2H, N-CH_2-CH_2-CH_2-CH_2-Ph), 2.61−2.71 (m, 4H, N-CH_2-CH_2-CH_2-CH_2-Ph and 4-H), 3.23−3.30 (m, 2H, 2-H and 5-H), 3.76 (s, 3H, OCH_3), 4.31 (d, J = 5.9 Hz, 1H, 1-H), 6.60 (d, J = 2.5 Hz, 1H, 6-H), 6.62 (dd, J = 8.0/2.7 Hz, 1H, 8-H), 6.99 (d, J = 8.0 Hz, 1H, 9-H), 7.15−7.19 (m, 3H, 2-H phenyl, 4-H phenyl and 6-H phenyl), 7.26−7.29 (m, 2H, 3-H phenyl and 5-H phenyl). A signal for the OH proton is not visible.

Methyl (*S*)-2-{*N*-[2-(3-Benzyloxyphenyl)ethyl]-*N*-(4-tosyl)-amino}propionate ((*S*)-23b). Under N_2 a solution of phenylethanol **22b** (5.77 g, 25.4 mmol) in THF (600 mL) was cooled to 0 °C. Then sulfonamide (*S*)-**12** (7.36 g, 28.6 mmol), Ph_3P (20.2 g, 76.1 mmol), and DIAD (14.7 mL, 76.1 mmol) were added and the mixture was stirred at 0 °C for 1 h and at rt for 16 h. The solution was diluted with *n*-hexane (700 mL) and the precipitate Ph_3P=O was removed by filtration. The solvent was evaporated in vacuum and the residue was purified by fc (8 cm, *n*-hexane/ethyl acetate 8:2, 65 mL, R_f = 0.35). Colorless oil, yield 13.9 g (71%). $[\alpha]_D$ −23.4 (*c* 1.01, CH_3OH). $C_{26}H_{29}NO_5S$ (467.3). ^{1}H NMR ($CDCl_3$): δ (ppm) = 1.36 (d, J = 7.3 Hz, 3H, N-CH-CH_3), 2.40 (s, 3H, Ph-CH_3), 2.84−2.91 (m, 1H, Ph-CH_2-CH_2-N), 2.99−3.06 (m, 1H, Ph-CH_2-CH_2-N), 3.22−3.30 (m, 1H, Ph-CH_2-CH_2-N), 3.41−3.46 (m, 1H, Ph-CH_2-CH_2-N), 3.48 (s, 3H, CO_2CH_3), 4.65 (q, J = 7.3 Hz, 1H, N-CH-CH_3), 5.05 (s, 2H, O-CH_2-Ph), 6.78−6.84 (m, 3H, 2-H phenyl, 4-H phenyl and 6-H phenyl), 7.20 (t, J = 7.5 Hz, 1H, 5-H phenyl), 7.26−7.45 (m, 7H, CH aromatic), 7.70 (d, J = 8.3 Hz, 2H, 2-H tosyl and 6-H tosyl).

(*S*)-7-Benzyloxy-2-methyl-3-(4-tosyl)-2,3,4,5-tetrahydro-3-benzazepin-1-one ((*S*)-25b) and (*S*)-9-Benzyloxy-2-methyl-3-(4-tosyl)-2,3,4,5-tetrahydro-3-benzazepin-1-one ((*S*)-26b) and 6-Benzyloxy-1-methyl-2-(4-tosyl)-1,2,3,4-tetrahydroisoquinoline (27b). Under N_2 a solution of the acid (*S*)-**24b** (4.77 g, 10.5 mmol) in CH_2Cl_2 (295 mL) was cooled to −15 °C. Then trifluoroacetic acid anhydride (5.56 mL, 39.4 mmol) was added and the mixture was stirred for 30 min at −15 °C. After addition of $SnCl_4$ (4.61 mL, 39.4 mmol), the mixture was stirred at −15 °C for 24 h. Water (150 mL) was added slowly, and the temperature was increased to rt. The aqueous layer was neutralized with 2 M NaOH, saturated with NaCl and extracted with CH_2Cl_2 (3 × 75 mL). The combined organic layers were dried (Na_2SO_4), concentrated in vacuum, and the residue was dissolved in acetone (180 mL). K_2CO_3 (5.44 g, 39.4 mmol) and benzyl bromide (1.56 mL, 13.1 mmol) were added, and the suspension was heated to reflux for 6 h. The mixture was filtered, concentrated in vacuum, and the residue was purified by fc (8 cm, *n*-hexane/ethyl acetate 7:3, 65 mL, R_f (**27b**) = 0.66 and R_f ((*S*)-**25b** and (*S*)-**26b**) = 0.34). (*S*)-**25b** and (*S*)-**26b** (R_f = 0.34): Colorless solid, yield 1.88 g (41%). **27b** (R_f = 0.66): Pale yellow resin, yield 855.8 mg (20%). $C_{25}H_{25}NO_4S$ (435.6). ^{1}H NMR ($CDCl_3$): δ (ppm) = 1.43 (d, J = 7.5 Hz, 3 × 0.95H, N-CH-CH_3●), 1.59 (d, J = 7.6 Hz, 3 × 0.05H, N-CH-CH_3□), 2.30 (s, 3 × 0.95H, Ph-CH_3●), 2.36 (s, 3 × 0.05H, Ph-CH_3□), 2.79−2.89 (m, 1H, 4-H), 2.95−3.07 (m, 1H, 5-H), 3.48 (ddd, J = 13.0/6.7/1.8 Hz, 0.95H, 5-H●), 3.61 (ddd, J = 13.3/6.7/1.9 Hz, 0.05H, 5-H□), 3.99−4.08 (m, 1H, 4-H), 4.76 (q, J = 7.5 Hz, 0.95H, 2-H●), 4.92 (q, J = 7.6 Hz, 0.05H, 2-H□), 5.06 (s, 2 × 0.95H, O-CH_2-Ph●), 5.08 (s, 2 × 0.05H, O-CH_2-Ph□), 6.60 (d, J = 7.8 Hz, 0.05H, 6-H□), 6.64 (d, J = 2.4 Hz, 0.95H, 6-H●), 6.71 (d, J = 8.5 Hz, 0.05H, 8-H□), 6.76 (dd, J = 8.5/2.5 Hz, 0.95H, 8-H●), 7.00 (d, J = 8.7 Hz, 2 × 0.05H, 3-H tosyl and 5-H tosyl□), 7.02 (d, J = 7.9 Hz, 2 × 0.95H, 3-H tosyl● and 5-H tosyl●), 7.13−7.24 (m, 4 × 0.05H, C-H aromatic□), 7.28 (d, J = 8.5 Hz, 0.95H, 9-H●), 7.32−41 (m, 6.85H, C-H aromatic). The ratio of regioisomers **25b**/**26b** is 95 (●) and 5 (□), respectively.

(1*S*,2*S*)-7-Benzyloxy-2-methyl-3-(4-tosyl)-2,3,4,5-tetrahydro-1*H*-3-benzazepin-1-ol ((*S*,*S*)-28) and (1*R*,2*S*)-7-Benzyloxy-2-methyl-3-(4-tosyl)-2,3,4,5-tetrahydro-1*H*-3-benzazepin-1-ol ((*R*,*S*)-28). Under N_2, $NaBH_4$ (0.55 g, 14.3 mmol) was added to a 95:5 mixture of (*S*)-**25b** and (*S*)-**26b** (3.11 g, 7.16 mmol) in CH_3OH (75 mL). After stirring for 20 h at rt, H_2O (30 mL) was added. The aqueous layer was extracted with CH_2Cl_2 (3 × 20 mL). The combined organic layers were dried (Na_2SO_4), concentrated in vacuum, and the residue was purified by fc (8 cm, *n*-hexane/ethyl acetate7:3, 65 mL, R_f ((*S*,*S*)-**28**) = 0.44, R_f ((*R*,*S*)-**28**) = 0.29). The potential product **29** was not isolated. (*S*,*S*)-**28** (R_f = 0.44): Colorless solid, mp 144 °C, yield 837.1 mg (27%). $[\alpha]_D$ −0.21 (*c* 0.80, $CHCl_3$, 8.3% ee). (*R*,*S*)-**28** (R_f = 0.29): Colorless solid, mp 151 °C, yield 1.18 g (38%). $[\alpha]_D$ +13.3 (*c* 1.01, $CHCl_3$, 2.1% ee).

(*S*,*S*)-**28**: $C_{25}H_{27}NO_4S$ (437.3). ^{1}H NMR ($CDCl_3$): δ (ppm) = 0.57 (d, J = 6.8 Hz, 3H, N-CH-CH_3), 1.64 (br s, 1H, OH), 2.38 (s, 3H, Ph-CH_3), 2.68 (dd, J = 14.5/5.5 Hz, 1H, 5-H), 2.80−2.96 (m, 2H, 4-H

DOI: 10.1021/acs.jmedchem.5b00897
J. Med. Chem. XXXX, XXX, XXX−XXX

and 5-H), 4.02−4.08 (m, 1H, 4-H), 4.35 (ddd, J = 6.9/2.4/0.9 Hz, 1H, 2-H), 5.00 (s, 2H, O-CH_2-Ph), 5.00−5.05 (m, 1H, 1-H), 6.68 (d, J = 2.6 Hz, 1H, 6-H), 6.82 (dd, J = 8.6/2.6 Hz, 1H, 8-H), 7.25 (d, J = 7.9 Hz, 2H, 3-H and 5-H tosyl), 7.27−7.31 (m, 1H, 4-H benzyl), 7.33−7.40 (m, 5H, 2-H, 3-H, 5-H, 6-H benzyl and 9-H), 7.68 (d, J = 8.3 Hz, 2H, 2-H and 6-H tosyl).

(*R,S*)-**28**: $C_{25}H_{27}NO_4S$ (437.3). ^{1}H NMR ($CDCl_3$): δ (ppm) = 0.69 (d, J = 6.7 Hz, 3H, N-CH-CH_3), 1.59 (br s, 1H, OH), 2.39 (s, 3H, Ph-CH_3), 2.57−2.62 (m, 1H, 5-H), 3.01 (ddd, J = 14.3/5.7/1.1 Hz, 1H, 4-H), 3.43−3.50 (m, 1H, 5-H), 4.06 (ddd, J = 14.5/5.7/2.4 Hz, 1H, 4-H), 4.44−4.51 (m, 2H, 1-H and 2-H), 5.00 (s, 2H, O-CH_2-Ph), 6.68−6.71 (m, 2H, 6-H and 8-H), 7.01 (d, J = 8.7 Hz, 1H, 9-H), 7.25 (d, J = 7.9 Hz, 2H, 3-H tosyl and 5-H tosyl), 7.27−7.32 (m, 1H, 4-H benzyl), 7.33−7.40 (m, 4H, 2-H benzyl, 3-H benzyl, 5-H benzyl and 6-H benzyl), 7.68 (d, J = 8.3 Hz, 2H, 2-H tosyl and 6-H tosyl). ^{13}C NMR ($CDCl_3$): δ (ppm) = 13.7 (1C, N-CH-CH_3), 21.7 (1C, Ph-CH_3), 37.3 (1C, C-5), 41.4 (1C, C-4), 54.4 (1C, C-2), 70.1 (1C, O-CH_2-Ph), 78.5 (1C, C-1), 111.7 (1C, C-8), 118.0 (1C, C-6), 127.1 (2C, C-2 tosyl and C-6 tosyl), 127.7 (2C, C-2 benzyl and C-6 benzyl), 128.2 (1C, C-4 benzyl), 128.8 (2C, C-3 benzyl and C-5 benzyl), 129.9 (2C, C-3 tosyl and C-5 tosyl), 130.8 (1C, C-9a), 132.4 (1C, C-9), 137.0 (1C, C-1 benzyl), 138.1 (1C, C-1 tosyl), 141.2 (1C, C-5a), 143.4 (1C, C-4 tosyl), 158.8 (1C, C-7).

(1*S*,2*S*)-7-Benzyloxy-2-methyl-2,3,4,5-tetrahydro-1*H*-3-benzazepin-1-ol ((*S,S*)-30). Mg (1.37 g, 56.9 mmol) was added to a solution of (*S,S*)-**28** (1.13 g, 2.58 mmol) in CH_3OH (130 mL). The reaction mixture was heated under reflux for 36 h. 2 M HCl (pH 3) was added, and the mixture was filtered. The solution was adjusted with 2 M NaOH to pH 10, the water layer was extracted with CH_2Cl_2 (5 × 50 mL), the organic layer was dried (Na_2SO_4), concentrated in vacuum, and the residue was purified by fc (6 cm, ethyl acetate/CH_3OH 95:5 + 2% *N,N*-dimethylethanamine, 30 mL, R_f = 0.23). Colorless solid, mp 175 °C, yield 438.1 mg (60%). $[\alpha]_D$ −0.90 (c 0.77, CH_3OH, 8.3% ee). $C_{18}H_{21}NO_2$ (283.4). ^{1}H NMR ($CDCl_3$): δ (ppm) = 0.96 (d, J = 6.9 Hz, 3H, N-CH-CH_3), 2.55 (ddd, J = 14.7/5.3/1.3 Hz, 1H, 5-H), 2.90 (ddd, J = 13.4/5.4/2.8 Hz, 1H, 4-H), 3.03−3.09 (m, 1H, 4-H), 3.27−3.34 (m, 2H, 2-H and 5-H), 4.37 (d, J = 5.4 Hz, 1H, 1-H), 5.04 (s, 2H, O-CH_2-Ph), 6.70−6.73 (m, 2H, 6-H and 8-H), 7.06 (d, J = 7.8 Hz, 1H, 9-H), 7.30−7.35 (m, 1H, 4-H benzyl), 7.37−7.44 (m, 4H, 2-H benzyl, 3-H benzyl, 5-H benzyl and 6-H benzyl). Signals for the OH-and NH-protons are not visible.

(1*S*,2*S*)-7-Benzyloxy-2-methyl-3-(4-phenylbutyl)-2,3,4,5-tetrahydro-1*H*-3-benzazepin-1-ol ((*S,S*)-31) and (1*R*,2*R*)-7-Benzyloxy-2-methyl-3-(4-phenylbutyl)-2,3,4,5-tetrahydro-1*H*-3-benzazepin-1-ol ((*R,R*)-31). A mixture of the secondary amine (*S,S*)-**30** (122.2 mg, 0.43 mmol), 1-chloro-4-phenylbutane (108.0 μL, 0.66 mmol), Bu_4NI (241.0 mg, 0.65 mmol), K_2CO_3 (301.0 mg, 2.18 mmol), and CH_3CN (20 mL) was heated to reflux for 72 h. The mixture was filtered, concentrated in vacuum, and the residue was purified by fc (3 cm, *n*-hexane/ethyl acetate 7:3 and 1% *N,N*-dimethylethanamine, 10 mL, R_f = 0.22). Colorless solid, mp 101 °C, yield 154.1 mg (86%), mixture of enantiomers (*S,S*)-**31** and (*R,R*)-**31** in the ratio 54:46. The enantiomer (*R,R*)-**30** was transformed in the same manner. The enantiomers (*S,S*)-**31** and (*R,R*)-**31** were separated on an analytical chiral HPLC (column Chiralpak IB, Chiral Technologies Europe, solvent *n*-hexane/ethanol/isopropanol 96:3:1, t_R ((*S,S*)-**31**) = 48.6 min, t_R ((*R,R*)-**31**) = 58.6 min).

(*S,S*)-**31** (t_R = 48.6 min): Colorless resin, $[\alpha]_D$ +1.33 (c 1.33, CH_2Cl_2, 98.8% ee).

(*R,R*)-**31** (t_R = 58.6 min): Colorless resin, $[\alpha]_D$ −2.00 (c 0.40, CH_2Cl_2, 98.4% ee).

Spectroscopic data of (*S,S*)-**31** and (*R,R*)-**31**: $C_{28}H_{33}NO_2$ (415.6). ^{1}H NMR ($CDCl_3$): δ (ppm) = 0.83 (d, J = 6.5 Hz, 3H, N-CH-CH_3), 1.49−1.59 (m, 2H, N-CH_2-CH_2-CH_2-CH_2-Ph), 1.61−1.69 (m, 2H, N-CH_2-CH_2-CH_2-CH_2-Ph), 2.63−2.91 (m, 8H, N-CH_2-CH_2-CH_2-CH_2-Ph, 4-H and 5-H), 3.00 (q, J = 6.7 Hz, 1H, 2-H), 4.88 (br s, 1H, 1-H), 5.04 (s, 2H, O-CH_2-Ph), 6.72 (d, J = 2.6 Hz, 1H, 6-H), 6.79 (dd, J = 8.3/2.6 Hz, 1H, 8-H), 7.17−7.20 (m, 3H, C-H aromatic), 7.25−7.44 (m, 8H, C-H aromatic). A signal for the OH proton is not visible.

(1*S*,2*S*)-2-Methyl-3-(4-phenylbutyl)-2,3,4,5-tetrahydro-1*H*-benzazepine-1,7-diol ((*S,S*)-32). Pd/C (10%, 50.0 mg) was added to a solution of the enantiomerically pure benzyl ether (*S,S*)-**31** (60.1 mg, 0.14 mmol) in absolute CH_3OH (6 mL), and the suspension was stirred under H_2 atmosphere (1 bar) for 1 h at rt. The catalyst was removed by filtration over Celite 535, the solvent was evaporated in vacuum, and the residue was purified by fc (2 cm, *n*-hexane/ethyl acetate 5:5 and 1% *N,N*-dimethylethanamine, 10 mL, R_f = 0.13). Colorless solid, mp 89 °C, yield 44.9 mg (95%). $[\alpha]_D$ −25.0 (c 0.5, CH_3OH, 98.8% ee). $C_{21}H_{27}NO_2$ (325.5). ^{1}H NMR ($CDCl_3$): δ (ppm) = 0.82 (d, J = 6.3 Hz, 3H, N-CH-CH_3), 1.49−1.68 (m, 4H, N-CH_2-CH_2-CH_2-CH_2-Ph), 2.58−2.77 (m, 7H, N-CH_2-CH_2-CH_2-CH_2-Ph, 4-H and 1 × 5-H), 2.82−2.89 (m, 1H, 5-H), 3.01 (q, J = 6.3 Hz, 1H, 2-H), 4.88 (br s, 1H, 1-H), 6.54 (d, J = 2.4 Hz, 1H, 6-H), 6.63 (dd, J = 8.2/2.5 Hz, 1H, 8-H), 7.16−7.19 (m, 4H, 9-H, 2-H phenyl, 4-H phenyl and 6-H phenyl), 7.26−7.29 (m, 2H, 3-H phenyl and 5-H phenyl). A signal for the OH proton is not visible.

Receptor Binding Studies. Cell Culture and Preparation of Membrane Homogenates for the GluN2B Assay. The assay for the GluN2B affinity has been reported in refs 25 and 26. Briefly, in the assay mouse L(tk−) cells stably transfected with the dexamethasone inducible eukaryotic expression vectors pMSG NR1a, pMSG NR2B in a 1:5 ratio were used. The transformed L(tk−) cells were grown in modified Earle's medium (MEM) containing 10% of standardized fetal calf serum (FCS, Biochrom AG, Berlin, Germany). The expression of the NMDA receptor at the cell surface was induced after the cell density of the adherent growing cells had reached approximately 90% of confluency. For the induction, the original growth medium was replaced by growth medium containing 4 μM dexamethasone and 4 μM ketamine (final concentration). After 24 h the cells were harvested by scraping and pelleted (10 min, 5000*g*, Hettich Rotina 35R centrifuge, Tuttlingen, Germany).

For the binding assay, the cell pellet was resuspended in phosphate buffer saline (PBS) buffer and the number of cells was determined using an improved Neubauer's counting chamber (VWR, Darmstadt, Germany). Subsequently, the cells were lysed by sonication (4 °C, 6 × 10 s cycles with breaks of 10 s; device, Soniprep 150, MSE, London, U.K.). The resulting cell fragments were centrifuged with a high performance cool centrifuge (20 000*g*, 4 °C, Sorvall RC-5 plus, Thermo Scientific). The supernatant was discarded and the pellet resuspended in a defined volume of PBS yielding cell fragments of approximately 500 000 cells/mL. The suspension of membrane homogenates was sonicated again (4 °C, 2 × 10 s cycles with a break of 10 min) and stored at −80 °C.

Performing the GluN2B Binding Assay. The competitive binding assay was performed with the radioligand [^{3}H]**1** (60 Ci/mmol, PerkinElmer) using standard 96-well-multiplates (Diagonal, Muenster, Germany). The thawed cell membrane preparation (about 20 μg of protein) was incubated with six different concentrations of test compounds, 5 nM [^{3}H]**1**, and Tris/EDTA buffer (5 mM/1 mM, pH 7.5) in a total volume of 200 μL for 120 min at 37 °C. The incubation was terminated by rapid filtration through the presoaked filtermats by using the cell harvester. After washing each well five times with 300 μL of water, the filtermats were dried at 95 °C. Subsequently, the solid scintillator was placed on the filtermat and melted at 95 °C. After 5 min, the solid scintillator was allowed to solidify at rt. The bound radioactivity trapped on the filters was counted in the scintillation analyzer. The nonspecific binding was determined with 10 μM unlabeled **1**. The K_d value of **1** is 7.6 nM.

Affinity toward the PCP Binding Site of the NMDA Receptor. The affinity toward the PCP binding site of the NMDA receptor was determined in receptor binding studies as described in refs 27 and 28 using [^{3}H](+)-MK-801 as radioligand.

Affinity toward σ_1 and σ_2 Receptors. The affinity toward σ_1 and σ_2 receptors was recorded in receptor binding studies as described in refs 29−31 using [^{3}H](+)-pentazocine and [^{3}H]di-*o*-tolylguanidine as radioligands, respectively.

Functional Activity. Glutamate induced cytotoxicity was determined as described recently.[32] Briefly, L(tk−) cells stably expressing either NR1-1a/NR2A (L12-G10 cells) or NR1-1a/NR2B

DOI: 10.1021/acs.jmedchem.5b00897
J. Med. Chem. XXXX, XXX, XXX−XXX

(L13-E6 cells) were preincubated with compounds (concentration range 1 nM to 10 μM, dissolved in DMSO) for 30 min. Then a mixture of (*S*)-glutamate and glycine (10 μM each) was added and the cells were further incubated for 4 h. Excitotoxicity was determined by detection of LDH release from the cells into the culture supernatants. In this assay 0% excitotoxicity is defined as LDH release in the presence of (*S*)-glutamate/glycine (10 μM each) and 100 μM ketamine, whereas 100% excitotoxicity is defined as LDH release after addition of (*S*)-glutamate/glycine in the absence of ketamine. Experiments were repeated at least three times with six replicates per test concentration. IC_{50} values were calculated using GraphPad Prism, version 5.0.

Computational Methods. General. The crystal structure of NMDA-GluN1b/GluN2B dimer in complex with **1** (3QEL)[6] was taken from the Protein Data Bank. All water molecules were removed except one water molecule (HOH415) located in the binding pocket. The crystal structure was then protonated using MOE modeling package (Chemical Computing Group)[33] and subsequently energy-minimized by applying Amber99 force field and the GB/SA continuum solvent model. A tethering constant of 100 kcal/(mol Å) was applied on the backbone during the minimization process.

Docking. MOE modeling software was used to generate the molecular structures of all compounds at the physiological pH. Initial ligand conformations were obtained by energy minimization using the MMFF94x force field implemented in MOE. The prepared structures were docked into ifenprodil binding pocket using the GOLD docking program (version 5.1);[34] a binding pocket of 6 Å around the cocrystallized ligand **1** was assigned, and the water molecule (HOH415) was kept in the binding pocket and set to toggle. Goldscore was chosen as the fitness function, and a maximum number of 10 GA runs for each compound was allowed. By use of this setup, the cocrystallized inhibitors could be correctly docked (rmsd below 1 Å) into the NMDA-GluN1b/GluN2B binding pocket.

Molecular Dynamics. The sander module in AMBER 12[35] was applied for the energy minimization steps while pmemd was utilized for the MD simulation. Particle-mesh-Ewald (PME) method was used to treat electrostatic interactions, and a cutoff radius of 8 Å was set for nonbonded interactions. Preparation of the input files was accomplished as follows: The general Amber force field (GAFF) with AM1-BCC charges and Amber03 force field, as implemented in AMBER 12, were applied to assign atom types to the ligand and the protein, respectively. The inhibitor−protein complexes were solvated in an octahedral box of TIP3P water with 13 Å between the complex surface and the box boundary, and counterions were added to neutralize the system.

The solvated complexes were then subjected to two steps of energy minimization: a 3000 steps minimization while keeping the protein fixed (2000 cycles of steepest descent followed by 1000 cycles of conjugate gradient), followed by 2000 cycles of minimization of the whole complex structure using 1000 steps steepest descent and subsequent 1000 steps conjugate gradient. The system was gradually heated to 300 K over 100 ps and then a 10 ns MD simulation was performed in the *NPT* ensemble (pressure of 1.0 bar and temperature of 300 K). During MD all covalent bonds involving H atoms were constrained using the SHAKE procedure, and the time step was set to 2 fs.

The root-mean-square deviation of the protein's backbone atoms and of the studied inhibitors was calculated using the first frame in the MD simulation as reference.

The hydrogen bonds formed between the inhibitors and neighboring protein residues in the binding pocket were analyzed using the program ptraj from AMBER 12 after extracting 1000 snapshots from the trajectories of the complex over the 10 ns MD simulation. The distance cutoff was set to 3.5 Å, and no angle cutoff was applied.

MM/GBSA Binding Energy Calculation. Estimation of the binding energy was accomplished using the molecular mechanics generalized Born surface area (MM/GBSA) method implemented in AMBER 12. A total of 500 frames obtained from the complex' trajectories were used for energy calculations, GB^{OBC} model was selected, and the entropy contributions were not included.

■ ASSOCIATED CONTENT

Supporting Information

Tables showing the optimization of the intramolecular Friedel−Crafts acylation, enantiomeric purity data, H-bond analyses, figures displaying chiral HPLC, docking of ifenprodil and all test compounds, rmsd plots of MD simulations, synthetic methods, physical, spectroscopic and purity data of all compounds, details of receptor binding studies, and a csv file containing molecular formula strings. The Supporting Information is available free of charge on the ACS Publications website at DOI: 10.1021/acs.jmedchem.5b00897.

■ AUTHOR INFORMATION

Corresponding Author

*Phone: +49-251-8333311. Fax: +49-251-8332144. E-mail: wuensch@uni-muenster.de.

Notes

The authors declare no competing financial interest.

■ ACKNOWLEDGMENTS

We are grateful to Prof. Dr. D. Steinhilber, Department of Pharmacy, University of Frankfurt, for donating us the L(tk−) cells stably expressing GluN1a/GluN2A and GluN1a/GluN2B receptor proteins. F.G. and T.W. acknowledge the expert technical assistance by Heidemarie Graf in performing the excitotoxicity assays. This work was funded by the Deutsche Forschungsgemeinschaft (Grant GRK 1143), which is gratefully acknowledged.

■ ABBREVIATIONS USED

NMDA, *N*-methyl-D-aspartate; AMPA, 2-amino-3-(3-hydroxy-5-methylisoxazol-4-yl)propionic acid; PCP, (1-phenylcyclohexyl)piperidine; DTG, di-*o*-tolylguanidine; mGlu, metabotropic glutamate receptor; iGlu, ionotropic glutamate recetptor; DIAD, diisopropyl azodicarboxylate; MD, molecular dynamics; MM/GBSA, molecular mechanics generalized Born surface area; rmsd, root-mean-square deviation; SEM, standard error of the mean; MEM, modified Earle's medium; FCS, fetal calf serum; PBS, phosphate buffer saline; PME, particle mesh Ewald

■ REFERENCES

(1) Bräuner-Osborne, H.; Egebjerg, J.; Nielsen, E. O.; Madsen, U.; Krogsgaard-Larsen, P. Ligands for glutamate receptors: design, and therapeutic potential. *J. Med. Chem.* **2000**, *43*, 2609−2645.

(2) Kew, J. N. C.; Kemp, J. A. Ionotropic and metabotropic glutamate receptor structure and pharmacology. *Psychopharmacology* **2005**, *179*, 4−29.

(3) Paoletti, P.; Neyton, J. NMDA recptor subunits: function and pharmacology. *Curr. Opin. Pharmacol.* **2007**, *7*, 39−47.

(4) Lodge, D. The history of the pharmacology and cloning of ionotropic glutamate receptors and the development of idiosyncratic nomenclature. *Neuropharmacology* **2009**, *56*, 6−21.

(5) Furukawa, H.; Singh, S. K.; Mancusso, R.; Gouaux, E. Subunit arrangement and function in NMDA receptors. *Nature* **2005**, *438*, 185−192.

(6) Karakas, E.; Simorowski, N.; Furukawa, H. Subunit arragement and phenylethanolamine binding in GluN1/GluN2B NMDA receptors. *Nature* **2011**, *475*, 249−253.

(7) Mony, L.; Kew, J. N. C.; Gunthorpe, M. J.; Paoletti, P. Allosteric modulators of NR2B-containing NMDA receptors: molecular

DOI: 10.1021/acs.jmedchem.5b00897
J. Med. Chem. XXXX, XXX, XXX−XXX

mechanisms and therapeutic potential. *Br. J. Pharmacol.* **2009**, *157*, 1301−1317.
(8) Paoletti, P.; Bellone, C.; Zhou, Q. NMDA receptor subunit diversity: impact on receptor properties, synaptic plasticity and disease. *Nat. Rev. Neurosci.* **2013**, *14*, 383−400.
(9) Layton, M. E.; Kelly, M. J., III; Rodzinak, K. J. Recent advances in the development of NR2B subtype-selective NMDA receptor antagonists. *Curr. Top. Med. Chem.* **2006**, *6*, 697−709.
(10) Wu, L.-J.; Zhou, M. Targeting the NMDA receptor subunit NR2B for the treatment of neuropathic pain. *Neurotherapeutics* **2009**, *6*, 693−702.
(11) Williams, K. Ifenprodil, a novel NMDA receptor antagonist: site and mechanism of action. *Curr. Drug Targets* **2001**, *2*, 285−298.
(12) Falck, E.; Begrow, F.; Verspohl, E.; Wünsch, B. Metabolism studies of ifenprodil, a potent GluN2B receptor antagonist. *J. Pharm. Biomed. Anal.* **2014**, *88*, 96−105.
(13) Borza, I.; Domány, G. NR2B selective NMDA antagonists: the evolution of the ifenprodil-type pharmacophore. *Curr. Top. Med. Chem.* **2006**, *6*, 687−695.
(14) Yurkewicz, L.; Weaver, J.; Bullock, M. R.; Marshall, L. F. The effect of the selective NMDA receptor antagonist traxoprodil in the treatment of traumatic brain injury. *J. Neurotrauma* **2005**, *22* (12), 1428−1443.
(15) Wessell, R. H.; Ahmed, S. M.; Menniti, F. S.; Dunbar, G. L.; Chase, T. N.; Oh, J. D. NR2B selective NMDA receptor antagonist CP-101,606 prevents levodopa-induced motor response alterations in hemi-parkinsonian rats. *Neuropharmacology* **2004**, *47*, 184−194.
(16) Tewes, B.; Frehland, B.; Schepmann, D.; Schmidtke, K.-U.; Winckler, T.; Wünsch, B. Design, synthesis, and biological evaluation of 3-benzazepin-1-ols as NR2B-selective NMDA receptor antagonists. *ChemMedChem* **2010**, *5*, 687−695.
(17) Tewes, B.; Frehland, B.; Schepmann, D.; Schmidtke, K.-U.; Winckler, T.; Wünsch, B. Conformationally constrained NR2B selective NMDA receptor antagonists derived from ifenprodil: Synthesis and biological evaluation of tetrahydro-3-benzazepine-1,7-diols. *Bioorg. Med. Chem.* **2010**, *18*, 8005−8015.
(18) Ordonez, M.; De La Cruz-Cordero, R.; Fernandez-Zertuche, M.; Munoz-Hernandez, M. A.; Garcia-Barradas, O. Diastereoselective reduction of dimethyl γ-[(N-p-toluenesulfonyl)amino]-β-ketophosphonates derived from amino acids. *Tetrahedron: Asymmetry* **2004**, *15*, 3035−3043.
(19) Chen, B. C.; Skoumbourdis, A. P.; Guo, P.; Bednarz, M. S.; Kocy, O. R.; Sundeen, J. E.; Vite, G. D. A facile method for the transformation of N-(tert-butoxycarbonyl) α-amino acids to N-unprotected α-amino methyl esters. *J. Org. Chem.* **1999**, *64*, 9294−9296.
(20) Swamy, C. C. K.; Kumar, N. N. B.; Balaraman, E.; Kumar, K. V. P. P. Mitsunobu and related reactions: advances and applications. *Chem. Rev.* **2009**, *109*, 2551−2651.
(21) Schläger, T.; Oberdorf, C.; Tewes, B.; Wünsch, B. Novel, one-pot procedure for the synthesis of 2-arylethanol derivatives. *Synthesis* **2008**, *2008*, 1793−1797.
(22) Duhamel, L.; Fouquay, S.; Plaquevent, J.-C. Ligand exchange in asymmetric reactions of lithium enolates: application to the deracemization of α-aminoacids. *Tetrahedron Lett.* **1986**, *27*, 4975−4978.
(23) Tewes, B.; Frehland, B.; Fröhlich, R.; Wünsch, B. Novel GluN2B selective NMDA receptor antagonists: relative configuration of 7-methoxy-2-methyl-tetrahydro-3-benzazepin-1-ols. *Acta Crystallogr., Sect. E*, submitted **2015**.
(24) Tewes, B.; Frehland, B.; Fröhlich, R.; Wünsch, B. Relative configuration of 7-benzyloxy-2-methyl-3-tosyltetrahydro-3-benzazepin-1-ol for the elucidation of the relative configuration of potent allosteric GluN2B selective NMDA receptor antagonists. *Acta Crystallogr., Sect. E*, submitted **2015**.
(25) Schepmann, D.; Frehland, B.; Lehmkuhl, K.; Tewes, B.; Wünsch, B. Development of a selective competitive receptor binding assay for the determination of the affinity to NR2B containing NMDA receptors. *J. Pharm. Biomed. Anal.* **2010**, *53*, 603−608.
(26) Benner, A.; Bonifazi, A.; Shirataki, C.; Temme, L.; Schepmann, D.; Quaglia, W.; Shoji, O.; Watanabe, Y.; Daniliuc, C.; Wünsch, B. GluN2B-selective *N*-methyl-D-aspartate (NMDA) receptor antagonists derived from 3-benzazepines: synthesis and pharmacological evaluation of benzo[7]annulen-7-amines. *ChemMedChem* **2014**, *9*, 741−751.
(27) Köhler, J.; Bergander, K.; Fabian, J.; Schepmann, D.; Wünsch, B. Enantiomerically pure 1,3-dioxanes as highly selective NMDA and σ_1 receptor ligands. *J. Med. Chem.* **2012**, *55*, 8953−8957.
(28) Banerjee, A.; Schepmann, D.; Köhler, J.; Würthwein, E.-U.; Wünsch, B. Synthesis and SAR studies of chiral non-racemic dexoxadrol analogues as uncompetitive NMDA receptor antagonists. *Bioorg. Med. Chem.* **2010**, *18*, 7855−7867.
(29) Meyer, C.; Neue, B.; Schepmann, D.; Yanagisawa, S.; Yamaguchi, J.; Würthwein, E.-U.; Itami, K.; Wünsch, B. Improvement of σ_1 receptor affinity by late-stage C-H-bond arylation of spirocyclic lactones. *Bioorg. Med. Chem.* **2013**, *21*, 1844−1856.
(30) Miyata, K.; Schepmann, D.; Wünsch, B. Synthesis and σ receptor affinity of regioisomeric spirocyclic furopyridines. *Eur. J. Med. Chem.* **2014**, *83*, 709−716.
(31) Hasebein, P.; Frehland, B.; Lehmkuhl, K.; Fröhlich, R.; Schepmann, D.; Wünsch, B. Synthesis and pharmacological evaluation of *like*- and *unlike*-configured tetrahydro-2-benzazepines with α-substituted benzyl moiety in 5-position. *Org. Biomol. Chem.* **2014**, *12*, 5407−5426.
(32) Rook, Y.; Schmidtke, K.-U.; Gaube, F.; Schepmann, D.; Wünsch, B.; Heilmann, J.; Lehmann, J.; Winckler, T. Bivalent beta-carbolines as potential multitarget anti-Alzheimer agents. *J. Med. Chem.* **2010**, *53*, 3611−3617.
(33) *Molecular Operating Environment (MOE)*, version 2012.10; Chemical Computing Group Inc. (1010 Sherbooke St. West, Suite No. 910, Montreal, QC, Canada, H3A 2R7), 2012.
(34) Verdonk, M. L.; Cole, J. C.; Hartshorn, M. J.; Murray, C. W.; Taylor, R. D. Improved protein-ligand docking using GOLD. *Proteins: Struct., Funct., Genet.* **2003**, *52*, 609−623.
(35) Case, D. A.; Darden, T. A.; Cheatham, T. E., III; Simmerling, C. L.; Wang, J.; Duke, R. E.; Luo, R.; Walker, R. C.; Zhang, W.; Merz, K. M.; Roberts, B.; Hayik, S.; Roitberg, A.; Seabra, G.; Swails, J.; Goetz, A. W.; Kolossváry, I.; Wong, K. F.; Paesani, F.; Vanicek, J.; Wolf, R. M.; Liu, J.; Wu, X.; Brozell, S. R.; Steinbrecher, T.; Gohlke, H.; Cai, Q.; Ye, X.; Wang, J.; Hsieh, M.-J.; Cui, G.; Roe, D. R.; Mathews, D. H.; Seetin, M. G.; Salomon-Ferrer, R.; Sagui, C.; Babin, V.; Luchko, T.; Gusarov, S.; Kovalenko, A.; Kollman, P. A. *AMBER 12*; University of California: San Francisco, CA, 2012.

DOI: 10.1021/acs.jmedchem.5b00897
J. Med. Chem. XXXX, XXX, XXX−XXX